INVESTIGATE THE DYNAMIC PERFORMANCE OF RENEWABLE ELECTRIC GENERATION SYSTEMS

Thesis submitted in partial fulfillment of the requirements for the award of the degree of

Master of Engineering
in
Power Systems & Electric Drives

Thapar University, Patiala

By
SYED ABDUL SHAKUR
Roll No: 800941022

Under the supervision of

Dr. Sanjay K. Jain
Associate Professor, EIED

JULY 2011

ELECTRICAL & INSTRUMENTATION ENGINEERING DEPARTMENT
THAPAR UNIVERSITY
PATIALA-147004

CERTIFICATE

I hereby certify that the work which is being presented in the thesis entitled, "**INVESTIGATE THE DYNAMIC PERFORMANCE OF RENEWABLE ELECTRIC GENERATION SYSTEMS**" in partial fulfillment of the requirement for the award of degree of Master of Engineering in ***Power Systems & Electric Drives*** submitted in Electrical & Instrumentation Engineering Department of Thapar University, Patiala, is an authentic record of my own work carried out under the supervision of **Dr. Sanjay K. Jain**, Associate Professor, EIED.

The matter presented in this thesis has not been submitted for the award of any other degree of this or any other university.

S. A. Shakur

(Syed Abdul Shakur)
Roll No: 800941022

It is certified that the above statement made by the student is correct and true to the best of my knowledge and belief.

Sanjay 12/07/2011

(Dr. Sanjay K. Jain)
Associate Professor
EIED, Thapar University
Patiala

Countersigned by

S. Ghosh 14/7/11

(Dr. Smarajit Ghosh)
Professor & Head
Electrical & Instrumentation Engg. Department
Thapar University,
Patiala

(Dr. S.K. Mohapatra)
Dean (Academic Affairs)
Thapar University,
Patiala

ACKNOWLEDGEMENT

On completion of my thesis work, it is my proud privilege to express my deep sense of gratitude towards **Dr. Sanjay K. Jain, Associate Professor, EIED** for his invaluable guidance, constant encouragement, suggestions, great patience, and continuous technical support which helped me to survive through crest and troughs of my thesis work and complete it successfully. It is a great privilege to work under him, who motivated me in every course of my work and made me believe in myself.

It is a great pleasure to express my special thanks to **Dr. Smarajit Ghosh, Professor and Head of EIED.**, for his suggestions and encouragement which helped me in completing this thesis work successfully. I also thank **Dr. Yaduvir Singh, P.G. Coordinator** and all faculty members of EIED for their encouragement.

Much appreciations is expressed to **Dr. Abhijit Mukherjee, Director, Thapar University, Dr. K.K. Raina, Deputy Director, Thapar University** and **Dr. S.K. Mohapatra, Dean of Academic Affairs** for providing moral support during my M.E. Thesis work.

I am very happy to express salutations to my parents because, my success, my failure, indeed everything I own, belongs to them. I would also like to express my deep affection and best wishes to my loving sister Miss. Syed Raheema and brother Mr. S. M. Siddique.

S. A. Shakur

Syed Abdul Shakur

800941022

ABSTRACT

The factors such as energy access, security and environmental considerations, and the increasing fuel prices have accelerated the adoption of affordable Renewable Electric Generation Systems (REGS). These systems decrease the dependency on imported fossil fuels and help in reducing the emissions of greenhouse gases. The renewable energy technologies, such as hydraulic turbine, solar cell, micro turbine, fuel cell, and wind turbine can deliver power with virtually zero emissions. The renewable generation is also referred by names such as distributed generation (DG), dispersed generation, embedded generation etc. The REGS are getting more importance as an alternate to large centralized generation plants, which is driven by the rapidly evolving liberalization and deregulation environments.

In this thesis, two renewable electric generation systems namely micro turbine (MT) system and fuel cell (FC) system has been studied. The MT system consists of micro turbine driven permanent magnet synchronous machine feeding to ac utility system via the power electronic interface. The FC system consists of solid oxide fuel cell is feeding to ac utility via the power conditioning unit interface. The detailed dynamic models of each component have been developed and the models are implemented under SIMULINK environment. The dynamic performance has been studied. The micro turbine operation during initial motoring and thereafter generating mode has been studied. The performance during grid connection and islanding is also studied. The active and reactive power variation for the connection of fuel cell system with ac utility has been studied.

TABLE OF CONTENTS

LIST OF FIGURES

LIST OF TABLES

CHAPTER 1

INTRODUCTION

1.1 OVERVIEW

The ever increasing demand for electrical power has created many challenges for the energy industry, which can affect the quality of the generated power in short and long terms [1]. The problem will imminently take a new form when limitation occurs in the transmission and distribution infrastructure. At the same time, the wide utilization of conventional fossil fuel-based sources will dramatically impact the quality and sustainability of life on earth. The realization of the problems associated with the conventional sources is defining a new set of power supply requirements that can better be served through renewable or distributed generation.

The centralized and regulated electric utilities have always been the major source of electric power production and supply. However, the increase in demand for electric power has led to the development of REGS which can complement the central power by providing additional capacity to the users. These are small generating units which can be located at the consumer end or anywhere within the existing electric system. The use of renewable generators can be beneficial to the consumers as well as the utility. The benefits to consumers include cost saving during peak demand charges, higher power quality and increased energy efficiency. The utilities can also benefit as it generally eliminates the cost needed for laying new transmission/distribution lines.

Although the, REGS or DG is being seen as solutions for both the short and long term problems [2-5], they are becoming more feasible as a result of falling price of small-scale power plants and the developments in data communications and control technologies. Renewable electric generation systems are expected to spread and have the potential to account for 20-30% of the distribution-system demand by 2020 [6, 7].

The REGS employ alternate resources such as micro-turbines, solar photovoltaic, hydraulic turbines, fuel cells and wind energy systems. The fuel cells (FCs) [8-11] and micro turbines (MTs) [12-15] are candidates to support the existing centralized power systems. MTs can produce low-cost low-emission electricity but at low efficiency which is limited by the combustion process. Fuel cells can essentially be described as batteries which never become discharged as long as hydrogen and oxygen are continuously provided.

Renewable electric generation provides many benefits to the power distribution network [16] which includes increase in system efficiency and the improvements in power system quality & reliability. To maximize these benefits, reliable generator units have to be connected at proper locations and with proper sizes [17]. However, such units will not generally be utility owned, which means that the adequate utilization of these units is not guaranteed [5]. Moreover, some renewable electric generator units, such as solar and wind, are variable energy sources and depend in their operation on weather conditions. Therefore, it is not ensured whether REGS will satisfy and meet all operation criteria in the power system. Some issues arise when these units are connected to power systems including the power quality, proper system operation and network protection [5].

In spite of the benefits of utilizing REGS, many technical and operational challenges have to be resolved before renewable electric generator becomes a routine. The lack of suitable control strategies for electrical networks with high penetration levels of generator units represents a problem for the futuristic systems. Also, the dynamic interaction between high-voltage parts of the network from one side and renewable electric generator units from the other side is an essential subject that needs extensive research. To simulate the behavior of modern electrical networks, suitable static and dynamic models for REGS units and the related interface devices are required. In addition, many topics of critical interest regarding the employment of renewable electric generator have to be investigated. Some of these topics are the overall system stability, the power quality and the interaction between the local regulators with those of the centralized energy plants.

1.2 LITERATURE SURVEY

A micro turbine generation (MTG) system comprises of a microturbine driving an electrical generator. The following paragraphs give a brief summary on the earlier work done on the microturbine part of the MTG system as well as a brief review of its electrical generator part.

Micro-turbines are small high-speed versions of conventional heavy-duty gas turbines. Hence the dynamic model of a conventional gas turbine, with relatively small thermodynamic constants, can be adopted to study the impacts of a microturbine on the overall system. A model of a heavy-duty gas turbine suitable was presented for use in dynamic power studies in [18]. The speed control, acceleration control, and fuel system controllers were used. Also, the developed model is suitable for both isolated and parallel operation. The gas turbine model was validated by comparing its dynamic performance with that of an operating gas turbine generation system [19].

The response of a combined cycle plant was simulated in [20] by using the gas turbine model presented in [19]. The system comprises of a gas turbine model and a steam turbine model which uses the waste heat from the gas turbine through a heat recovery system. This simulated (combined cycle) model can be used for system dynamic performance studies.

The influence of micro-turbines on distribution networks stability was studied in [21]. The transient and voltage stability of the system was examined. It is informed that the micro-turbines, acting as distributed resources, are capable of providing effective load following service in a distribution system. The proposed model of the microturbine was utilized to develop a control system with an adaptive controller for a fuel cell-microturbine hybrid power plant [22].

A complete model of the MTG system, was presented in [23]. It includes the power electronic interfacing and is suitable for transient analysis as well as simulation of unbalanced three-phase power system.

The electric generator used in a modern MTG system is usually a permanent magnet synchronous machine (PMSM). The detailed equations to model a PMSM have been summarized in [24].

The fuel cell is a fast growing technology and much research has been going on in this decade. Fuel cells are gaining much attention because of their light weight, compact size, low maintenance, and low acoustic and chemical emissions. They can serve as a potential source for electric power generation for stand-alone as well as for grid-tied applications.

A basic approach for fuel cell modeling suitable for renewable generation is summarized in [25]. The solid oxide fuel cell (SOFC) model [10, 28] was discussed by taking the temperature effect into account. A non-linear dynamic model of the SOFC that can be used for dynamic and transient stability studies was developed in [27]. A physically based model for tubular SOFC was developed in [28]. Simplified models of the SOFC have been presented in [29]-[32] considering constant cell temperature.

Fuel cells operate at low DC voltages and hence need to be boosted with the help of a DC-DC converter. Various topologies such as the H-bridge series resonant buck and boost converters have been presented in [33]. A DC-DC converter with a closed loop pulse width modulation (PWM) control strategy is described in [35].

DC-AC inverter converts the DC power of the fuel cell system into AC power for stand alone as well as grid connected applications. The voltage source inverter (VSI) plays a vital role in interfacing the fuel cell-DC-DC system with the utility grid. Various control strategies have been proposed for the VSI in [34], [36]-[39]. A real and reactive power control using dq transformation has been employed in [36]. The controllers based on PWM control, using [37] hysteresis control was discussed in [37]. The power conditioning system, including the DC/DC and DC/AC converters are presented in [38]. The case studies for the control of grid connected fuel cells for transient stability enhancement have been presented in [39].

1.3 OBJECTIVE OF WORK

The objective of the present work is to study the modeling and simulate the dynamic performance of various renewable energy generation systems based on micro turbine driven permanent magnet synchronous machine and solid oxide fuel cell. The work also has been carried out to investigate the behavior of independent systems comprising microturbine and fuel cell system.

1.4 ORGANIZATION OF THESIS

The work carried out in this thesis has been summarized in five chapters The **Chapter 1** briefs the overview, literature review, objectives of work and organization of the thesis. The **Chapter 2** deliberates on renewable electric generation. It introduces microturbine and fuel cells as Renewable Electric Generation Systems. The **Chapter 3** discusses about the micro turbine and its model. The **Chapter 4** deliberates on fuel cell system and the Model of solid oxide fuel cell and its power conditioning unit. The conclusions and the scope of further work are detailed in **Chapter 5**.

CHAPTER 2

RENEWABLE ELECTRIC GENERATION

2.1 RENEWABLE ELECTRIC GENERATION SYSTEMS

Renewable electric generation system is defined as the integrated or standalone utilization of renewable resources through small, modular electric generation units near the end user terminals [7]. The renewable electric generator may include any generation integrated into distribution system, commercial and residential back up generation, standalone onsite generators and generators installed by the utility for voltage support or other reliability purposes.

Today, new advances in power generation technologies and new environmental regulations encourage a significant increase of renewable electric generation resources around the world. Renewable electric generation systems (REGS) have mainly been used as a standby power source for critical businesses. For example, most hospitals and office buildings had stand-by diesel generators as an emergency power source for use only during outages. However, the diesel generators were not inherently cost-effective, and produce noise and exhaust that would be objectionable on anything except for an emergency basis. On the other hand, environmental-friendly renewable electric generation systems such as fuel cells, micro turbines, biomass, wind turbines, hydro turbines or photovoltaic arrays can be a solution to meet both the increasing demand of electric power and environmental regulations due to green house gas emission.

Fig. 2.1 and Fig. 2.2 show the future trends of electric utility industry. As illustrated in these figures, the currently competitive REGS units will be constructed on a conventional distribution network, instead of large central power plants because the REGS can offer improved service reliability, better economics and a reduced dependence on the local utility.

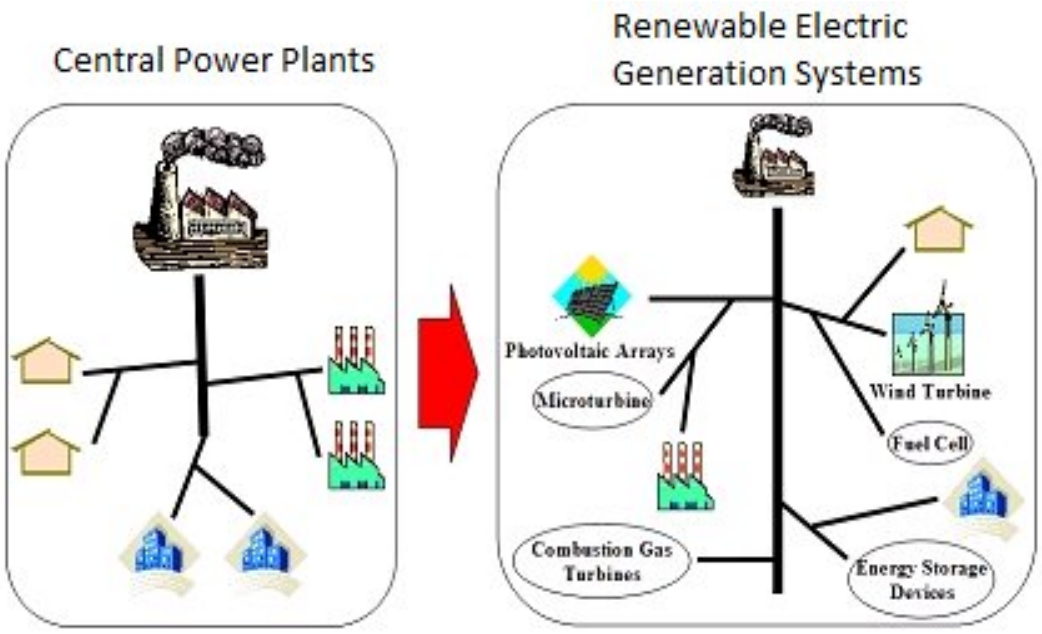

Fig. 2.1 A large central power plant and renewable electric generation systems

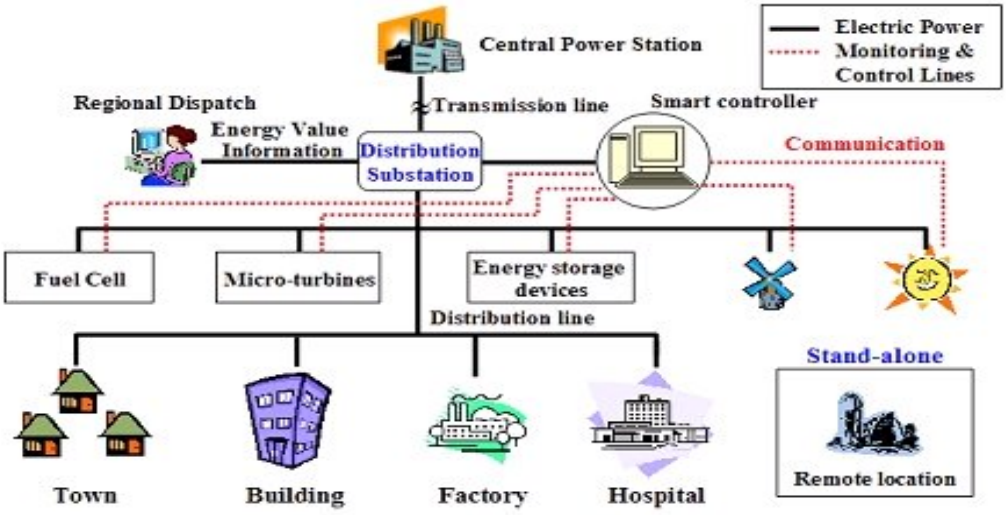

Fig. 2.2 Electric system with REGS

Recently, the use of renewable electric generation systems under the 500 kW level is rapidly increasing due to technology improvements in small generators, power electronics, and energy storage devices. Efficient clean fossil-fuels technologies such as micro-turbines, fuel-cells, and environmental-friendly renewable energy technologies such

as biomass, solar/photovoltaic arrays, small wind turbines and hydraulic turbines, are growingly used for new renewable electric generation systems.

In many applications, renewable electric generation technology can provide valuable benefits for both the consumers and the electric distribution systems [16]. The small size and the modularity of REGS encourage their utilization in a broad range of applications. The downstream location of REGS in distribution systems reduces energy losses and allows utilities to postpone upgrades to transmission and distribution facilities. The benefits of utilizing REGS can be summarized as follows:

- Improving availability and reliability of utility system
- Voltage support and improved power quality
- Reduced operating cost and lower losses
- The expenditures to upgrade the transmission and distribution are postponed or avoided
- Possibility of cogeneration applications
- Emission reduction
- Saving during peak hours

Renewable electric generation system can be used for different applications due to their small size, modularity and location in power systems. The main applications of REGS include the following fields [7]:

- Generating the base load power, as in the case of variable energy renewable energy sources
- Providing additional reserve power at peak load intervals
- Providing emergency or back up power to increase the stability and reliability of important loads
- Supplying remote loads separated from the main grid system
- Supporting the voltage and reliability by providing power services to the grid
- Cooling and heating purposes

It is also possible to use REGS to cover the load demand most of the time. In this case, renewable electric generation system has to be connected to a local grid for backup power. Another possibility is to use energy storage devices to ensure the continuity of supplying the load.

2.2 MICRO-TURBINE SYSTEM

The small gas-fired micro-turbines in the 25-500 kW that can be mass-produced at low cost have been more attractive due to the competitive price of natural gas, low installation and maintenance costs. It takes very clever engineering and use of innovative design (e.g. air bearing, recuperation) to achieve reasonable efficiency and costs in machines of lower output. A big advantage of these systems is small-sized because these technologies mainly use high-speed turbines (50,000-120,000 RPM) with air foil bearings. Therefore, micro-turbines are one of the most promising of the renewable electric generation technologies for applications today. Fig. 2.3 shows a block diagram of micro-turbine system that consists of air compressor, recuperator, combustor, turbine, generator, and a PCU (Power Conditioning Unit) and its features are summarized below [23].

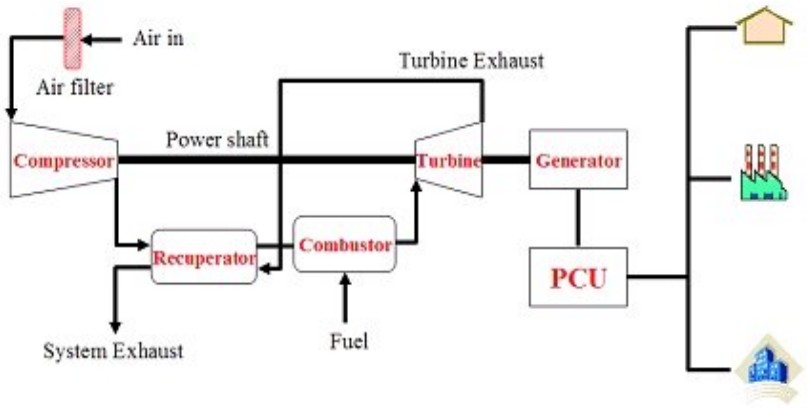

Fig. 2.3 Block diagram of micro-turbine system

2.3 FUEL CELL SYSTEM

Fuel cells are also well used for renewable electric generation applications, and can essentially be described as batteries which never become discharged as long as hydrogen and oxygen are continuously provided. The hydrogen can be supplied directly, or indirectly produced by reformer from fuels such as natural gas, alcohols, or gasoline. Each unit ranges in size from 1-250 kW or larger MW size. Even if they offer high efficiency and low emissions, today's costs are high. Phosphoric acid fuel cell is commercially available in the range of the 200 kW, while solid oxide and molten carbonate fuel cells are in a pre-commercial stage of development. The possibility of using gasoline as a fuel for cells has resulted in a major development effort by the automotive companies. The recent research work about the fuel cells is focused towards the polymer electrolyte

membrane (PEM) fuel cells. Fuel cells in sizes greater than 200 kW hold promise beyond 2005, but residential size fuel cells are unlikely to have any significant market impact any time soon. Fig. 2.4 shows a block diagram of fuel cell system which consists of a reformer, fuel cell stack and a PCU [26-28].

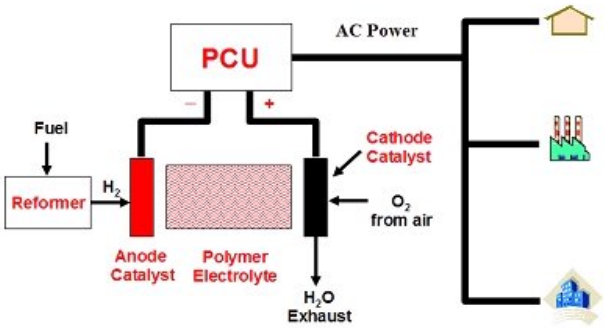

Fig. 2.4 Block diagram of fuel cell system

2.4 COMPARISON OF REGS

A comparison of currently competitive REGS technologies namely MTG and Fuel cells is given in Table 1. In the past, the electric utility industry did not offer suitable options that were suited for a wide range of consumer needs, and most utilities offered at best two or three combinations of reliability and price. However, the modern types of REGS give commercial electric consumers various options in a wider range of reliability-price combinations. For these reasons, the REGS will be very likely to thrive in the next 20 years in particular. REGS technologies will have a much greater market potential in areas such as developing countries whose electricity costs are high and unreliable.

Table 1: Comparison of various REGS Technologies

Technology	Micro Turbine	Fuel Cells
Output Generated	25-500 KW	1 kW-10 MW
Installed Cost ($/kW)	1,200-1,700	1,000-5,000
Electrical Efficiency	20-30 %	30-60 %
Overall Efficiency	80-85 %	80-85 %
Fuel Type	Natural gas, Hydrogen, Bio gas	Hydrogen, Natural gas, Propane

CHAPTER 3

MODELING AND PERFORMANCE OF MICRO TURBINE SYSTEM

3.1 INTRODUCTION

The renewable electric generation system based on microturbine technology is becoming more potential and viable distributed energy source in the recent years. This is due to their salient features such as high operating efficiency, ultra low emission levels, low initial cost and small size [15]. The microturbine generation system (MTG) produce power in the range of 25-500 kW and can be operated in stationary or mobile, remote or interconnected with the utility grid.

The basic components of a micro turbine are the compressor, combustor, turbine generator and recuperate as shown in Fig. 3.1. It operates on the same principles as traditional gas turbines. Air is drawn into compressor, where it is pressurized and forced into the cold side of recuperate. Here exhaust heat is used to preheat the air before it enters the combustion chamber. The combustion chamber then mixes the heated air with fuel and burns it. This mixture expands through the turbine, which drives the compressor and generator.

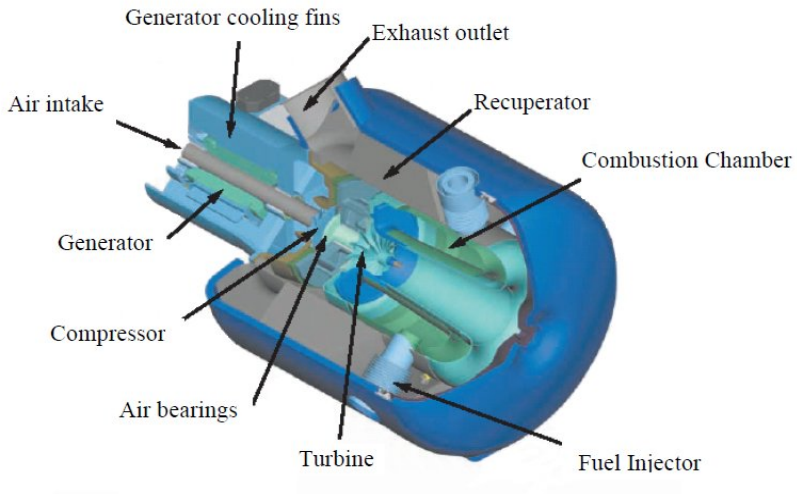

Fig 3.1 Construction of micro turbine unit

There are two types of micro turbine designs available, based on position of compressor turbine and generator. Fig. 3.2 (a) shows a high speed single shaft design with

the compressor and turbine mounted on the same shaft along with the permanent magnet synchronous generator. The generator generates power at very high frequency ranging from 1500 to 4000 Hz. The high frequency voltage is first rectified and then inverted to a normal AC power at 50 or 60 Hz. Another design is shown in Fig. 3.2 (b) in which the turbine on the first shaft directly drives the compressor while a power turbine on the second shaft drives the gearbox and conventional electrical generator (usually induction generator) producing 60 Hz power. The two-shaft design features more moving parts but does not require complicated power electronics to convert high frequency AC power output to 60 Hz.

Microturbine turbo-machinery is based on single-stage radial flow compressors and turbines. This offers highest efficiency in various size ranges; whereas moderate to large size gas turbines use multi-stage axial flow turbines and compressors.

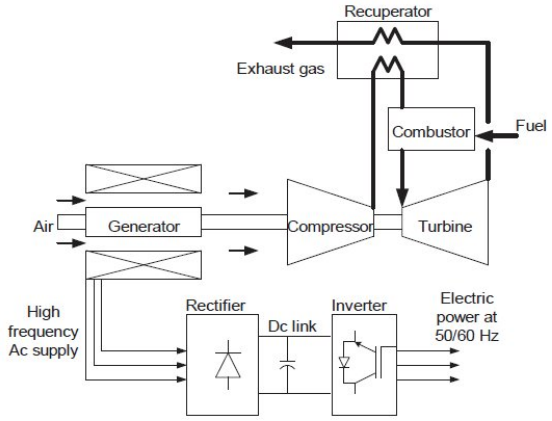

(a) ***Single shaft MTG system***

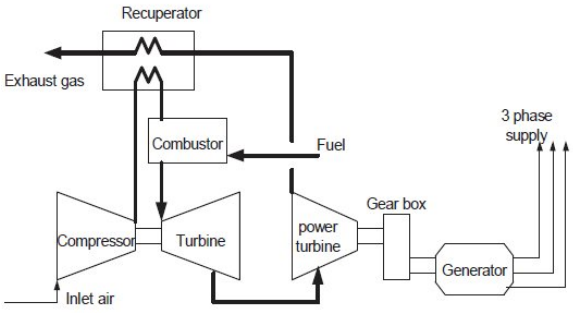

(b) ***Split shaft MTG system***

Fig. 3.2 Schematic diagram of MTG system

In a microturbine, the turbo-compressor shaft generally turns at high rotational speed as high as 1, 20,000 rpm based on the power rating. The microturbine utilizes gas foil bearings (air bearings) for high reliability, low maintenance and safe operation. This needs minimum components and no liquid lubrication is necessary to support the rotating group. Recuperators are heat exchangers that use the hot exhaust gas of the turbine (typically around 1,200ºF) to preheat the compressed air (typically around 300ºF) going into the combustor. This reduces the fuel needed to heat the compressed air to turbine inlet temperature. With recuperator microturbine efficiency can go above 80%.

The newly developed MTs have the following advantages [15]:

- low installation and infrastructure requirements, about 700 $/kW
- low maintenance costs, about 0.005$/kWh
- smaller and lighter than other engines with the same capacity
- reliable and durable due to the simplicity of the structure
- fuel flexibility since they can run on a variety of fuels including natural gas, diesel, ethanol, propane and gasoline
- high efficiency, with fuel energy to electricity conversion reaching 25%-30%
- possibility of cogeneration by using the waste heat recovery, which could achieve overall energy efficiency levels reaching 75%
- environmental superiority of MTs operating on natural gas

Microturbine generation system can be used for a wide range of applications [15]. These are

- Base load, Peak shaving and Stand-alone power
- Combined Heat and Power
- Resource Recovery
- UPS and Stand by Services

Base load, peak shaving and stand-alone power: Microturbine based renewable electric generation system can operate in parallel with grid or with any other generation source. The microturbine can augment utility supply during peak load periods, thus increasing power reliability and reducing or eliminating peak demand charges. Shaving peaks will increase overall system efficiency which will reduce investments in traditional generation, bulk transmission, and distribution facilities. Shaving peaks will also enable the utility to serve incremental load growth in areas where there is a shortage of substation

and/or distribution feeder capacity. The Microturbine can provide prime power generation where the electric utility grid is not readily available or where service is unreliable.

Combined Heat and Power: Cogeneration, or combined heat and power (CHP) generation refers to the process of utilizing the heat produced by a combustion engine as energy output. During normal operation, microturbine produces significant quantities of high-temperature exhaust that can be easily integrated with a heat exchanger and a hot water loop to produce valuable energy output. From a cost-benefit perspective, this yields a significant saving compared to heating fuel and purchasing power. When the heat energy is utilized, overall system fuel efficiency can range between 70% to 90%.

Resource Recovery: Flared gases often have low-energy yield or high contents of corrosive "sour" (hydrogen sulphide, or H_2S) gas, making them an infeasible fuel source for conventional generators. Microturbine, on the other hand has no problem operating exclusively on low-energy gases. Microturbine can also be used in oil and gas recovery applications. With the ability to convert unprocessed casing gas that contains up to 7% corrosive H_2S gas, microturbine can eliminate the need for flaring. At the same time, their power output reduces or eliminates the need for additional electricity sources.

UPS and Stand by Services: The microturbine technology can be integrated into a wide variety of products and systems. Uninterruptible power supplies, all-in-one combined heat and power systems, and welding machines are just a few examples for original equipment manufacturing applications.

3.2 MODELING OF MTG SYSTEM

As shown in Fig. 3.3, the integrated MTG system consists of

- Microturbine
- Permanent magnet synchronous machine
- Machine and grid side converters
- Control and filter

The modeling of individual components is described in this section.

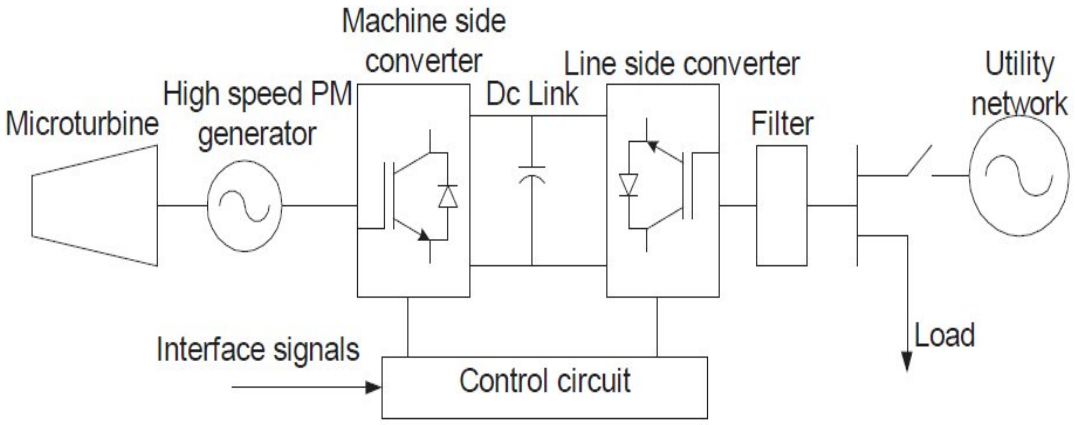

Fig. 3.3 MTG system with back to back converter interface

3.2.1 MODELING OF MICROTURBINE

The control functions of the microturbine are: speed control acting under part load conditions, temperature control acting as an upper output power limit, and acceleration control to prevent over speeding. The output of these control function blocks are all inputs to a least value gate (LVG), whose output is the lowest of the three inputs and results in the least amount of fuel to the compressor-turbine as shown in Fig. 3.4. This figure shows the per-unit representation of a microturbine, along with its control systems [18]. Each subsystem of the microturbine is discussed in the following subsections.

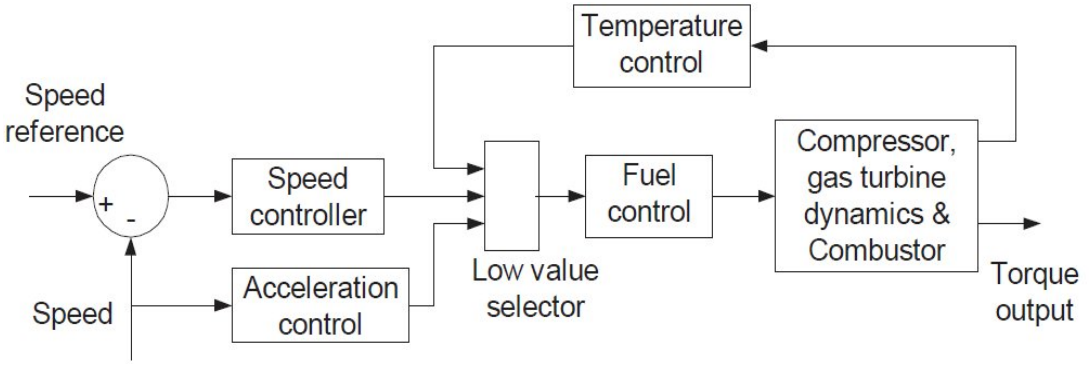

Fig. 3.4. Block diagram of Microturbine system with controls.

Speed and Acceleration Control: The speed control operates on the speed error formed between a reference (one per-unit) speed and the MTG system rotor speed. It is the primary means of control for the microturbine under part load conditions. Speed control is usually modeled by using a lead-lag transfer function [18], or by a PID controller [22]. In this work a lead lag transfer function has been used to represent the speed controller, as

shown in Fig. 3.5. In this figure K is the controller gain, T1 (T2) is the governor lead (lag) time constant, and Z is a constant representing the governor mode (droop or isochronous). A droop governor is a straight proportional speed controller in which the output is proportional to the speed error. An isochronous speed controller is a proportional-plus-reset speed controller in which the rate of change of the output is proportional to the speed error.

Acceleration control: The acceleration control is used primarily during turbine startup to limit the rate of the rotor acceleration prior to reaching operating speed. If the operating speed of the system is close to its rated speed, the acceleration control could be eliminated in the modeling [18].

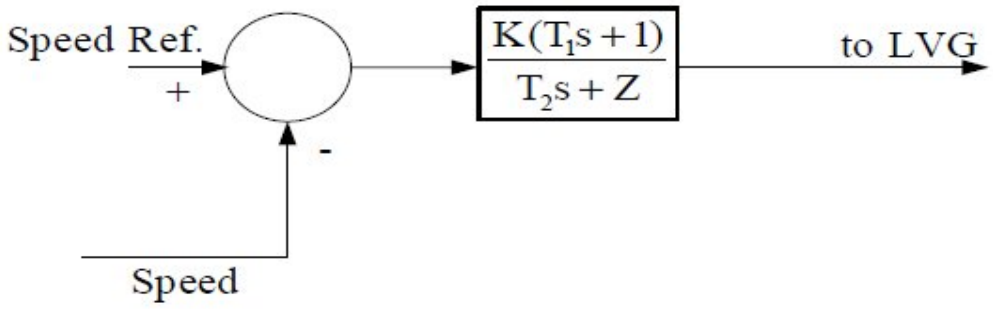

Fig. 3.5 Speed controller for the Microturbine

As mentioned in Fig. 3.5 Speed controller parameters are specified as *K*=25, *T1*=0.4, *T2*=1.0, *Z*=3.

Fuel System: The fuel system consists of the fuel valve and actuator. The fuel flow out from the fuel system results from the inertia of the fuel system actuator and of the valve positioner [18], [22], whose equations are given below.

The valve positioner transfer function is:

$$E_1 = \frac{K_v}{T_v s + c} F_d \tag{3.1}$$

And the fuel system actuator transfer function is:

$$Wf = \frac{K_f}{T_f s + c} E_1 \tag{3.2}$$

In (3.1) and (3.2), K_v (K_f) is the valve positioner (fuel system actuator) gain, T_v ,T_f are the valve positioner and fuel system actuator time constants, c is a constant, F_d and E_1 are the input and outputs of the valve positioner and Wf is the fuel demand signal in p.u.

The output of the LVG, V_{ce}, represents the least amount of fuel needed for that particular operating point and is an input to the fuel system. Another input to the fuel system is the per-unit turbine speed N (limited by the acceleration control). The per-unit value for V_{ce} corresponds directly to the per-unit value of the mechanical power on turbine at steady-state. The fuel flow control as a function of V_{ce} is shown in Fig. 3.6.

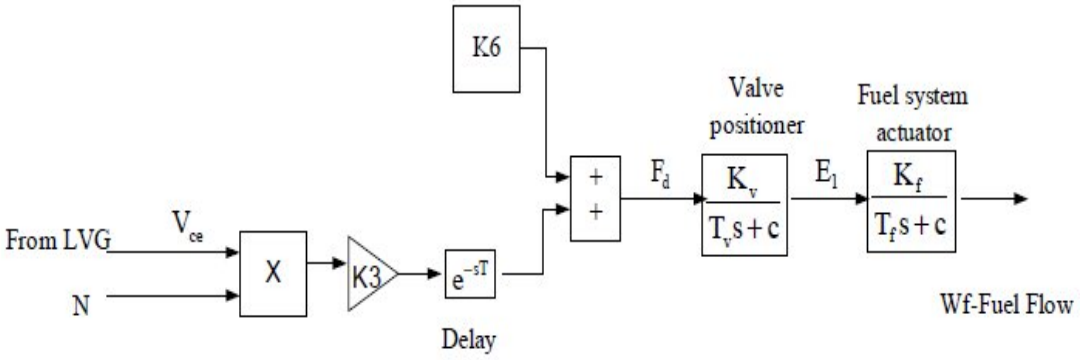

Fig. 3.6 Block diagram of the Fuel system

The value of Vce is scaled by the gain K3 (K3= (1-K6)), then delayed and offset by the minimum amount of fuel flow K6 to ensure continuous combustion process in the combustion chamber. K6 is essentially the minimum amount of fuel flow at no-load, rated speed.

As mentioned in Fig. 3.6 Fuel system parameters are specified as *Kv*=1, *Tv*=0.05, *c*=1, *K3*=0.77, *K6*=0.23, *Kf*=1, *T*=0, *Tf*=0.04.

Compressor-Turbine: The compressor-turbine is the heart of the microturbine and is essentially a linear, nondynamic device (with the exception of the rotor time constant) [18]. There is a small transport delay TCR, associated with the combustion reaction time, a time lag TCD, associated with the compressor discharge volume and a transport delay TTD , for transport of gas from the combustion system through the turbine.

The block diagram of the compressor-turbine package is shown in Fig. 3.7. In this figure both the torque and the exhaust temperature characteristics of the single-shaft gas turbine are essentially linear with respect to fuel flow and turbine speed and are given by the following equations [18]:

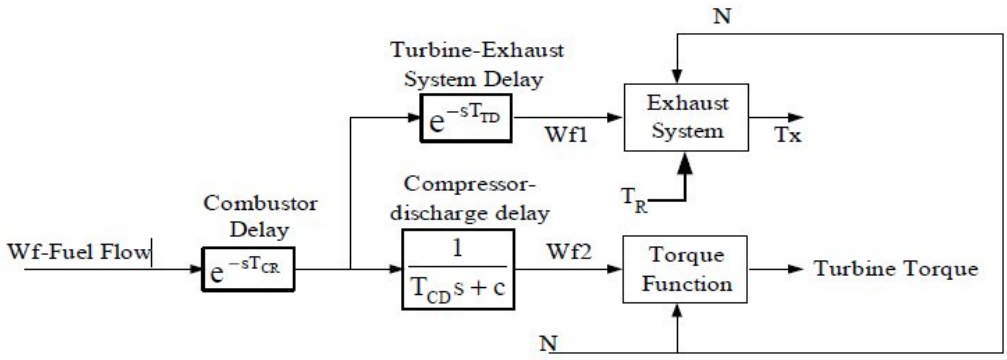

Fig. 3.7 Compressor-Turbine package of a microturbine

$$Torque = K_{HHV}(W_{f2} - 0.23) + 0.5(1-N)(Nm) \tag{3.3}$$

$$ExhaustTemp, T_X = T_R - 700(1-W_{f1}) + 550(1-N)(^\circ F) \tag{3.4}$$

where KHHV is a coefficient which depends on the enthalpy or higher heating value of the gas stream in the combustion chamber and TR is the reference temperature [18], [19]. The KHHV and the constant 0.23 in the torque expression cater for the typical power/fuel rate characteristic, which rises linearly from zero power at 23% fuel rate to the rated output at 100% fuel rate.

The input to this subsystem is the p.u. fuel demand signal Wf and outputs are the p.u. turbine torque and exhaust temperature (°F).

As mentioned in Fig. 3.7 Compressor-turbine combination parameters are specified as *TCR=0.01, TTD=0.04, TCD=0.2, KHHV=1.2.*

Temperature Control: Temperature control is the normal means of limiting the gas turbine output power at a predetermined firing temperature, independent of variation in ambient temperature or fuel characteristics. The fuel burned in the combustor results in turbine torque and in exhaust gas temperature. The exhaust temperature is measured using a series of thermocouples incorporating radiation shields as shown in the block diagram of the temperature controller (Fig. 3.8). In Fig. 3.8, Tt is the temperature controller

integration rate and T3, T4 are time constants associated with the radiation shield and thermocouple, respectively. K4 and K5 are constants associated with radiation shield and T5 is the time constant associated with temperature controller. The output from the thermocouple is compared with a reference temperature, which is normally higher than the thermocouple output. This forces the output of the temperature control to stay on the maximum limit permitting the dominance of speed control through the LVG (Fig. 3.4). When the thermocouple output exceeds the reference temperature, the difference becomes negative, and the temperature control output starts decreasing. When this signal (Fig. 3.4) becomes lower than the speed controller output, the former value will pass through the LVG to limit the turbine's output, and the turbine operates on temperature control. The input to the temperature controller is the exhaust temperature (Tx) and the output is the temperature control signal to the LVG [18], [19].

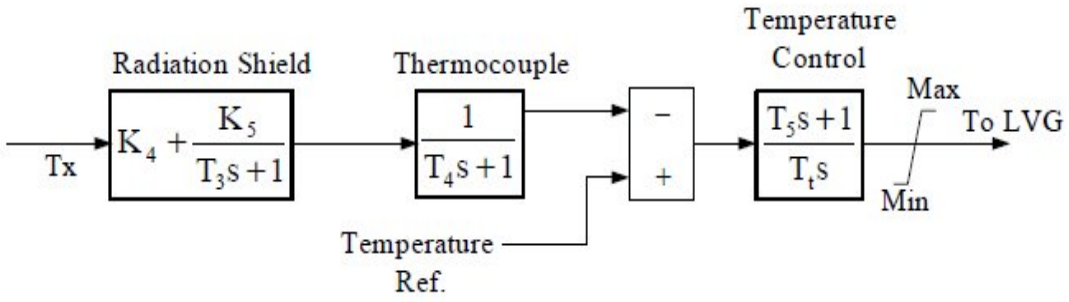

Fig. 3.8 Temperature controller

As mentioned in Fig. 3.8 Temperature controller parameters are specified as *K4*=0.8, *K5*=0.2, *T3*=15, *T4*=2.5, *T5*=3.3, *Tt*=450 °F, *TR*=950 °F.

The block diagram of microturbine along with its control is shown in Fig. 3.3 [26]. This consists of fuel, speed, acceleration and temperature control along with the combustor and turbine dynamics. The implementation of microturbine model using Simulink of the Matlab is shown in Fig 3.9.

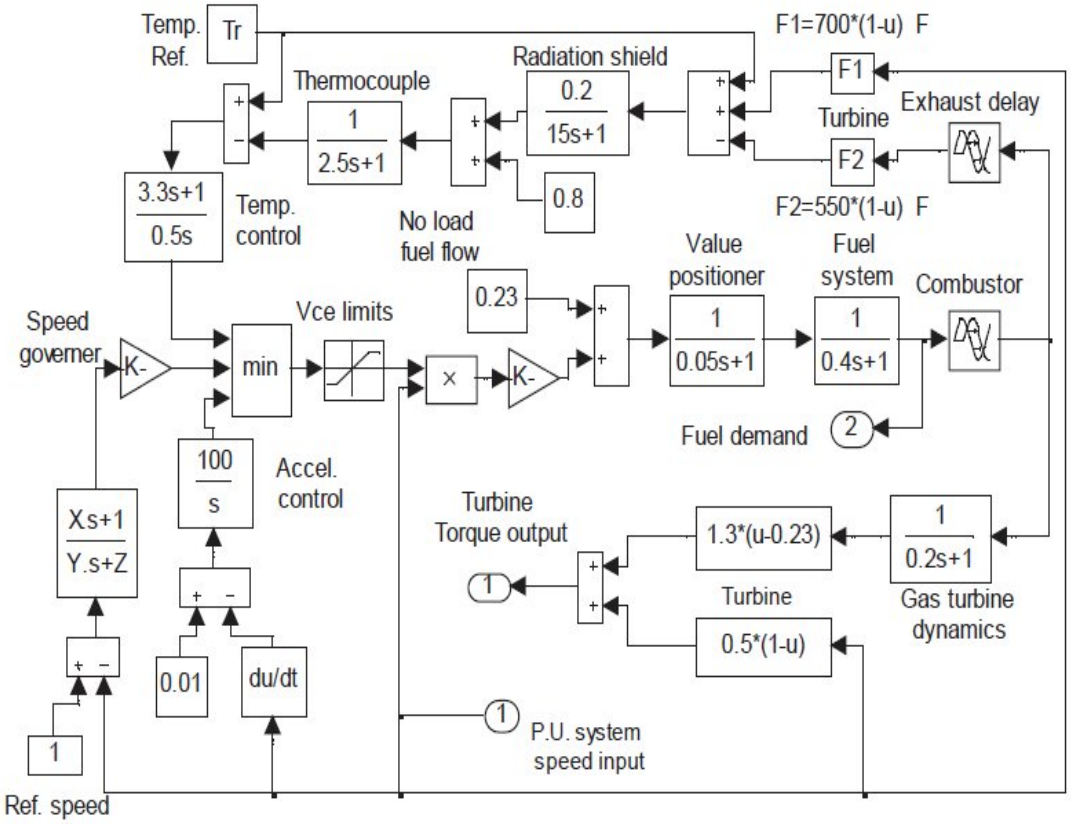

Fig. 3.9 Simulink model of the microturbine

3.2.2 PERMANENT MAGNET SYNCHRONOUS MACHINE (PMSM)

Microturbine produces electrical power via a high-speed generator directly driven by the turbo-compressor shaft. Small gas turbines benefit in particular when the gearbox that reduces the shaft speed to the speed of conventional electrical machines is eliminated, as is the case with the single-shaft designs considered here. The result is a more efficient, compact and reliable machine and the shaft speed is normally above 30,000 rev/min and may exceed 100,000 rev/min. High energy permanent magnets and high yield-strength materials like neodymium-iron-boron (NdBFe) or Samarium-cobalt magnets have proved very suitable for high-speed electrical machines [24].

In the following sections the equivalent circuit of a permanent magnet synchronous machine (PMSM) is presented.

In a permanent magnet synchronous machine, the dc field winding of the rotor is replaced by a permanent magnet. The advantages are elimination of filed copper loss, higher power density, lower rotor inertia, and more robust construction of the rotor. The

drawbacks are loss of flexibility of field flux control and possible demagnetization. The machine has higher efficiency than an induction machine, but generally its cost is higher [24].

dq Axis Representation of a PMSM. In a PMSM, the permanent magnets are glued on the rotor in surface sinusoidal magnet machine (SPM), and are mounted inside the rotor in case of an interior or buried magnet synchronous machine (IPM). The stator has three phase sinusoidal winding, which creates a synchronously rotating air gap flux. If the machine is rotated by a prime mover, the stator windings generate balanced three-phase sinusoidal voltages. The dq axis representation of a permanent magnet synchronous machine (for a balanced system the 0-axis quantities are equal to zero).

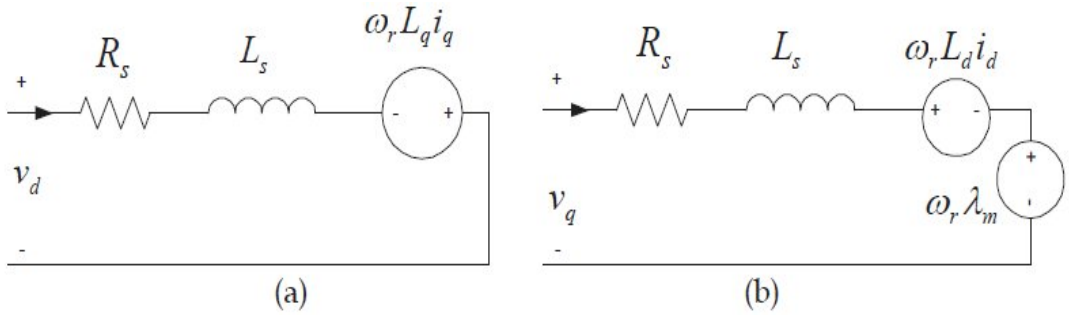

Fig. 3.10 dq-axis equivalent circuit model of the PMSM a) d-axis b) q-axis

The *dq*-axis equivalent circuit model of PMSM is shown in Fig. 3.10 The PMSM drive modeling is done with the assumption of sinusoidal distributed windings, saturation is neglected, **e**ddy currents and hysteresis losses are negligible [41]. With these assumptions the stator *dq* equations of the PMSM in the rotor reference frame are:

$$V_d = R_s i_d + L_d \frac{di_d}{dt} - p\omega_r L_q i_q \tag{3.5}$$

$$V_q = R_s i_q + L_d \frac{di_q}{dt} + p\omega_r L_d i_d + pw_r \phi_m \tag{3.6}$$

Where, the stator resistance is denoted by *Rs,* the *d*-axis and *q*-axis inductances are *Ld* and *Lq* respectively, *Φm* is the flux linkage due to the permanent magnets, *vd* and vq are *dq* axis voltages. In the *dq*-frame, the expression for electro-dynamic torque becomes:

$$T_e = 1.5\, p(\phi_m i_q + (L_d - L_q) i_q i_d) \tag{3.7}$$

The equation for motor dynamics can be given as:

$$\frac{d}{dt}\omega_r = \frac{1}{J}(T_e - F\omega_r - T_M) \tag{3.8}$$

$$\frac{d}{dt}\theta_r = \omega_r \tag{3.9}$$

$$\begin{bmatrix} v_q \\ v_d \\ v_o \end{bmatrix} = \frac{2}{3}\begin{bmatrix} \cos\theta_r & \cos(\theta_r - 120) & \cos(\theta_r + 120) \\ \sin\theta_r & \sin(\theta_r - 120) & \sin(\theta_r + 120) \\ 1/2 & 1/2 & 1/2 \end{bmatrix}\begin{bmatrix} v_a \\ v_b \\ v_c \end{bmatrix} \tag{3.10}$$

$$\begin{bmatrix} v_a \\ v_b \\ v_c \end{bmatrix} = \begin{bmatrix} \cos\theta_r & \sin\theta_r & 1 \\ \cos(\theta_r - 120) & \sin(\theta_r - 120) & 1 \\ \cos(\theta_r + 120) & \sin(\theta_r + 120) & 1 \end{bmatrix}\begin{bmatrix} v_q \\ v_d \\ v_o \end{bmatrix} \tag{3.11}$$

Where p is the number of pole pairs, Te is the electromagnetic torque, F is combined viscous friction of rotor and load, ωr is the rotor speed, and J is the moment of inertia, θr is rotor angular position and Tm is shaft mechanical torque. The d, q variables are obtained from a, b, c variables through the Park transform given in (3.10) and a, b, c variables are obtained from the d, q variables through the inverse of the Park transform given in (3.11).

Note that the signs for the generated torque Te and shaft torque Tshaft are positive for motor operation and negative for generator operation.

3.2.3 MACHINE SIDE CONVERTER CONTROL

Fig. 3.11 shows the Machine side converter controller implemented in Simulink of the Matlab. The commanded speed ωref is pre-calculated according to the turbine output power and set to the optimum speed [42]. Based on the speed error the commanded q axis reference current $iqref$ is determined through the speed controller [26].

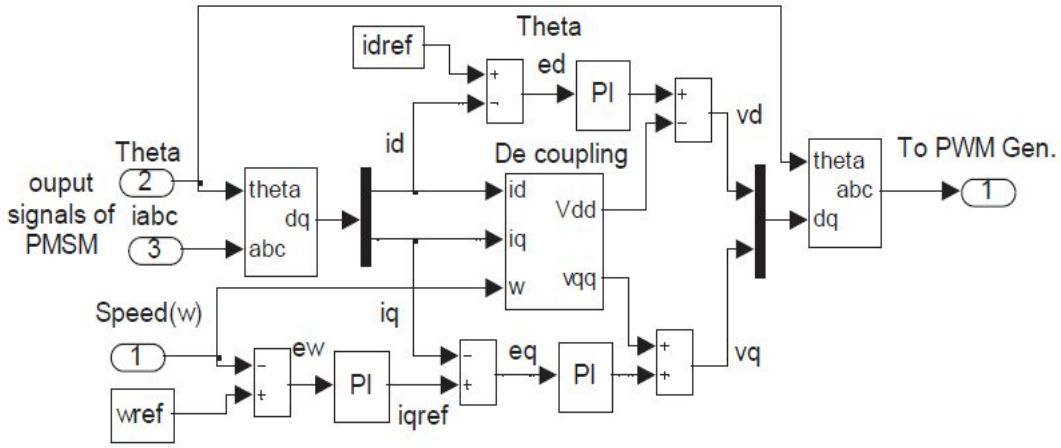

Fig. 3.11 Machine side converter controller implemented in simulink

In this system the following PI controller is employed as the speed controller.

$$i_{qref} = K_{p\omega} e_{\omega} + K_{i\omega} \int e_{\omega} dt \tag{3.12}$$

Where $K_{p\omega}$ and $K_{i\omega}$ are the proportional and integral gains of the speed controller respectively while e_{ω} is the error between the reference speed and measured speed. The commanded optimal d-axis current i_{dref} is obtained from the maximum allowed phase voltage and phase current constraints of the drive, which are given in (3.13) and (3.14). These constraints depend upon the machine rating and DC link voltage.

$$v_d^2 + v_q^2 \le v_{\max}^2 \tag{3.13}$$

$$i_d^2 + i_q^2 \le i_{\max}^2 \tag{3.14}$$

Using the above constraints and neglecting the voltage drop due to the stator resistance, the optimal d-axis current for a non salient for a non salient PMSM (L_d=L_q) can be obtained as:

$$i_d = \frac{\frac{V_{\max}^2}{\omega^2} - L_q^2 I_{\max}^2 - \lambda_m^2}{2 L_d \lambda_m} \tag{3.15}$$

Considering the relationship $i_{\max}^2 = i_d^2 + i_q^2$ the optimal d-axis current can be given as a function of the q-axis current i_q, as:

$$i_d = -\frac{\lambda_m}{L_d} + \sqrt{\left(\frac{V_{\max}}{\omega L_d}\right)^2 - \left(\frac{L_q}{L_d} i_q\right)^2} \tag{3.16}$$

Based on the currnet error the d-q axis reference voltage are determine by PI controllers, as given in (3.17) and (3.18).

$$v_d = K_{pi} e_{id} + K_{Ii} \int e_{id} dt - \omega_r L_q i_q \tag{3.17}$$

$$v_q = K_{pi} e_{iq} + K_{Ii} \int e_{iq} dt + \omega_r (L_d i_d + \lambda_m) \tag{3.18}$$

Where K_{pi} and K_{Ii} are the proportional and integral gains of the controller respectively. $e_{id} = i_{dref} - i_d$ is he d-axis current error and $e_{iq} = i_{qref} - i_q$ is the q-axis current error. The decoupling terms $\left(-\omega_r L_q i_q\right)$ and $\left(\omega_r \left(L_d i_d + \lambda_m\right)\right)$ are used in (3.17) and (3.18) respectively for the independent control of d and q-axis currents. The commanded dq-axis voltages $\left(v_d, v_q\right)$ are transformed into a, b, c variables $\left(v_a, v_b, v_c\right)$ and given to the PWM generator to generate the gate pulse for machine side converter.

3.2.4 LINE SIDE CONVERTER CONTROL

The objective of the supply-side converter is to keep the DC-link voltage constant, regardless of the magnitude and direction of the rotor power. A vector control approach is used here, with the reference frame oriented along the stator (or supply) voltage vector position [26].

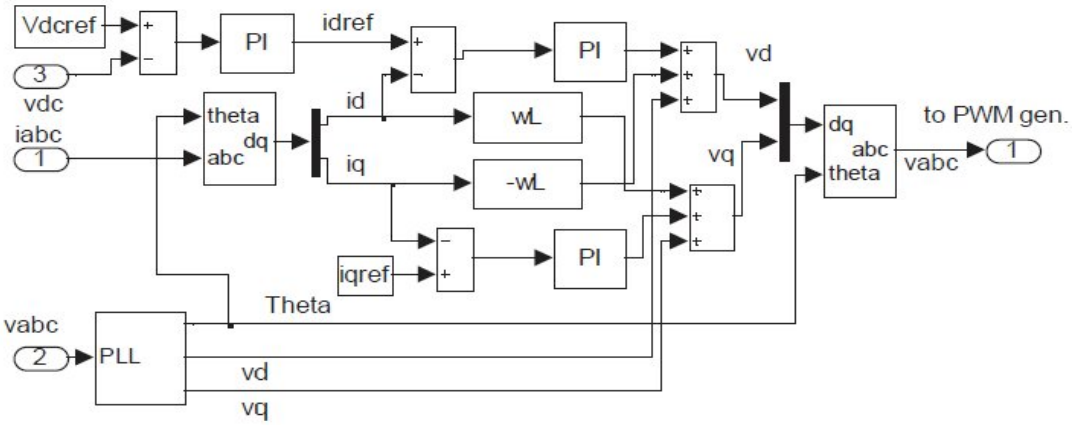

Fig. 3.12. Grid side Converter controller.

3.2.5 GRID AND ISLANDING MODES

Grid connected mode: The PQ control strategy with DC link voltage control is employed for grid connected operation of MTG system. In this scheme the power injected to the grid is regulated by controlling the injected current. The control structure for grid-connected mode operation of MTG system is shown in Fig. 3.12. The standard PI-controllers are used to regulate the currents in the *dq* synchronous frame in the inner control loops as they have satisfactory behavior in regulating DC variables, as well as filtering and controlling can be easily achieved. Another PI controller is used in the outer loop to regulate the capacitor voltage in accordance with the current injected in to the grid. Its output is the reference for the active current PI controller. In order to obtain only a transfer of active power, the *iq* current reference is set to zero. And also to have independent control of the current components *id* and *iq* the decoupling voltage components are added to the output of current PI controllers [26].

Converter voltages can be given as:

$$v_a(t) = \sqrt{\frac{2}{3}} V \cos(\omega t) \tag{3.19 a}$$

$$v_b(t) = \sqrt{\frac{2}{3}} V \cos\left(\omega t - \frac{2\pi}{3}\right) \tag{3.19 b}$$

$$v_c(t) = \sqrt{\frac{2}{3}} V \cos\left(\omega t - \frac{4\pi}{3}\right) \tag{3.19 c}$$

Dq component in synchronous reference frame with decoupling terms can be represented as:

$$u_d = Ri_d + L_d \frac{di_d}{dt} + v_d - \omega L_q i_q \tag{3.20}$$

$$u_q = Ri_q + L_q \frac{di_q}{dt} + v_q + \omega L_q i_q \tag{3.21}$$

Where, the dq currents are controlled by means of the right choice of the dq converter side voltages. Two PI regulators are command a PWM modulator to generate the voltage that should control the current.

Islanding mode: The islanding mode operation of single shaft MTG system requires a control different from that of grid connected mode. In this mode, the system has already been disconnected from the utility. Therefore the voltage and frequency is no longer regulated by it. Thus the output voltages are to be controlled in terms of amplitude and frequency which leads to control of the reactive and active power flow [26].

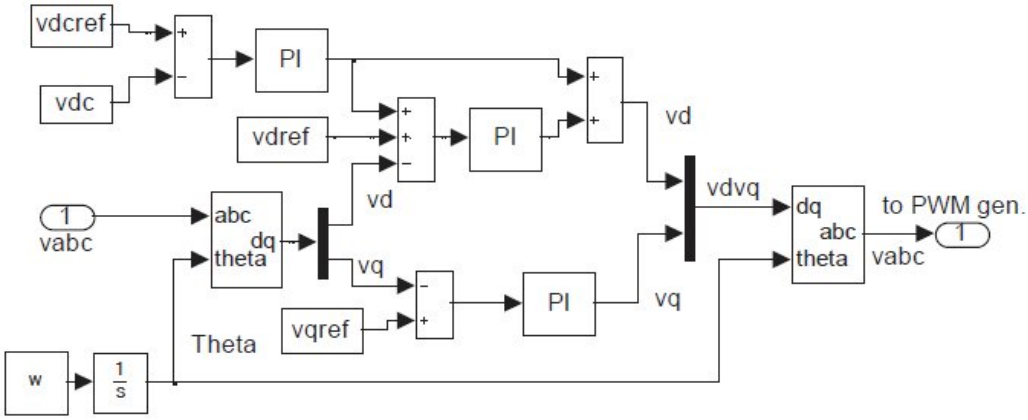

Fig 3.13 Control Structure for Islanding mode operation

This is done by controlling the amplitude and frequency of the modulating input-signal to the PWM inverter. The control structure for islanding mode is depicted in Fig. 3.13. It consists of output voltage and DC link voltage PI controllers. The output voltage controllers control the output voltage with a minimal influence from nature of the load currents or load transients. A standard PI controller operating in the synchronously rotating coordinate system where, *vq* is kept to zero is used. The DC voltage PI controller controls the DC voltage level based on the reference. For fast response the output of the DC voltage controller is feed forwarded to the voltage controller output. The DC link voltage controller acts only when the DC link voltage is below the reference and it lowers the voltage reference of the main voltage controller in order to avoid inverter saturation. The frequency control is done by integrating the constant reference frequency ω and using it for coordinate transfer of the voltage components from *abc* to *dq* and vice versa. In islanding mode, when there is more generation than the load demand the DC link voltage becomes higher than the reference. For this case damping chopper control is implemented. By activating this control excess energy stored in the Dc –link is dissipated in the damping resistor and hence maintain the Dc link voltage constant. A proportional controller is used to control the duty cycle of the chopper. In practice, batteries are used to sore the excess energy.

One of the important requirements in the interconnection design of the power electronic converter interfaced renewable electric generation system is that of synchronization to the utility system. Synchronism of converter control with the grid is achieved by using a PLL [43]. The Simulink block diagram of the PLL used in this work is shown in Fig. 3.14, where γ is the grid phase angle, V_x and V_y are the grid voltage components in the stationary reference frame. The philosophy of the PLL is that the sine of the difference between grid phase angle γ and inverter phase angle θ can be reduced to zero using a PI-controller, thus locking the inverter phase to the grid with small arguments $\left(\sin(\gamma-\theta)=(\gamma-\theta)=\Delta\theta\right)$. The output of the PI controller is the inverter output frequency that is integrated to obtain the inverter phase angle θ. In order to improve the dynamic response at startup, the nominal frequency of the grid, ω_o is feed forwarded to the output of the PI controller. The major disadvantage of the three phase PLL is its sensitivity to grid voltage unbalance. Some attempts are made to extend this method for unbalanced voltages based on Symmetrical components [24].

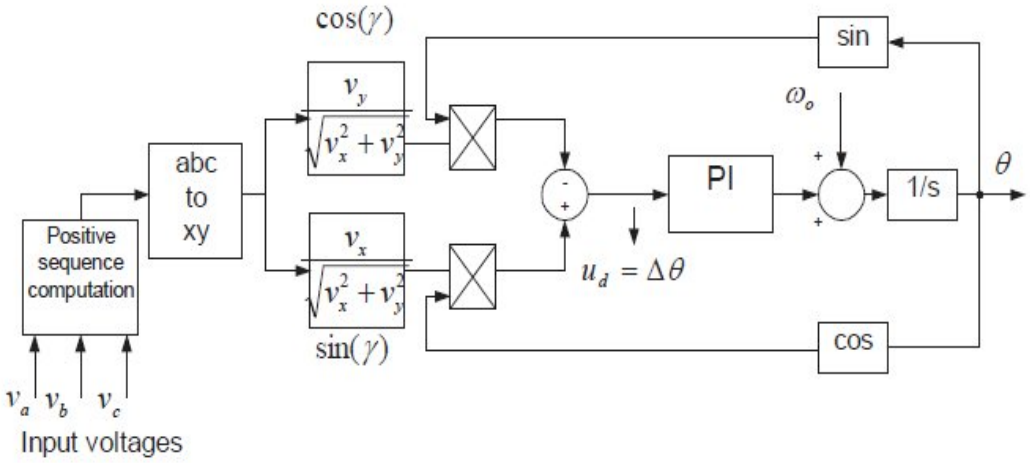

Fig 3.14. PLL implemented in simulink

3.3 SIMULATION OF MTG

Figure 3.15 shows the simulation model implemented in the SimPowerSystems of the MATLAB to study the performance of the MTG system operation in grid connected mode [40]. The utility network, to which the MTG system is connected, is represented by a 3 phase sinusoidal source with its impedance. The series RL filter is used at the grid side of the MTG system. The simulation parameters of the model are given in Table 2 [26].

The micro turbine generation system takes per unit speed of the PMSM as input. The torque output of the microturbine is given as an input mechanical torque (T_m) to the PMSM. The direction of the torque T_m, is positive during motoring mode and made negative during generating mode of the PMSM. The machine side converter controller takes the rotor angle speed and 3 phase stator current signals of the PMSM as inputs. In all the presented cases the voltage across the capacitor is zero, at the starting of simulation. During the start up, the PMSM operates as a motor to bring the turbine to a speed of 30,000 rpm. In this case power flows from the grid to MTG system.

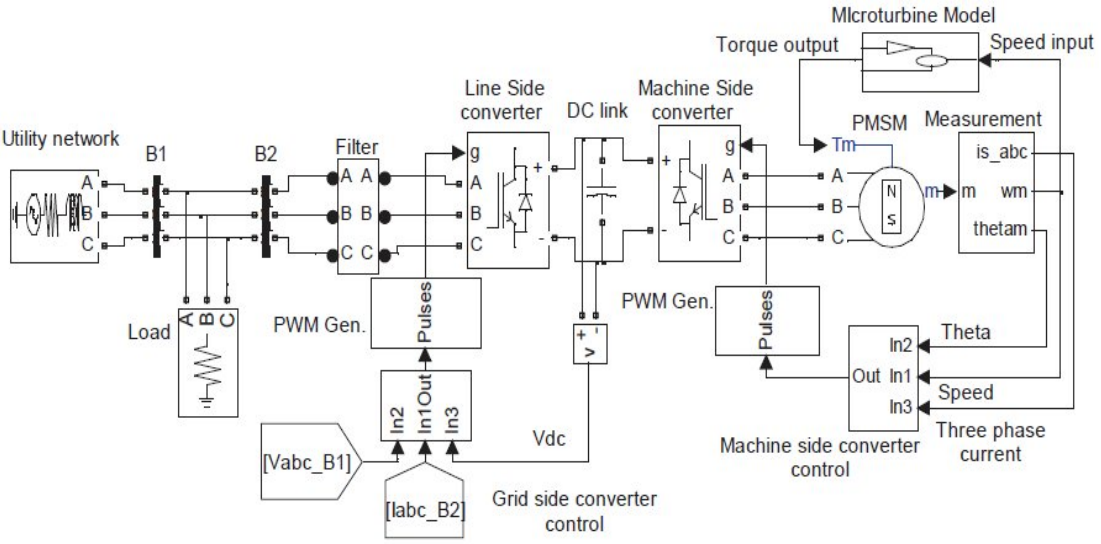

Fig 3.15. Matlab/SimPowerSystems implementationof MTG system connected to grid

Table 2 Simulation parameters for the model shown in Fig 3.15

Grid parameters	480V, 60Hz, R_s = 0.4Ω and L_s = 2Mh
Filter parameters	L = 0.97mH, R = 0.21 Ω
Switching Frequency	Grid side converter = 8KHz Machine side converter = 20KHz
DC link capacitance	500µF
PI controllers sampling time	100µsec
PMSM parameters	480V, 30kW, 1.6KHz, 96000rpm, R_s = 0.25Ω, Lq = Ld = 0.0006875H
Microturbine parameters	Gain (K) = 25, X = 0.4, Y = 0.05 and Z = 1

3.4 RESULTS AND DISCUSSIONS

The model used for the performance of MTG system is shown in Fig. 3.15. The MTG system is connected to 3-ϕ utility having voltage as 480 volt and local load of 10 kW. The Speed (rad/sec) – Time characteristics of microturbine is shown in Fig. 3.16.

The Fig. 3.16 shows the microturbine reaches the set value of speed of 3100 in 0.35 sec Till 0.4 sec. MTG absorbs 5.2 kW power from grid as shown in Fig. 3.17. This suggests that microturbine system is operating in motoring mode. When PMSM is switched to Generating mode as shown in fig. 3.16, the power flows from MTG system to Grid. In generating mode MTG Generates 14 kW of power to the Grid as shown in fig. 3.17.

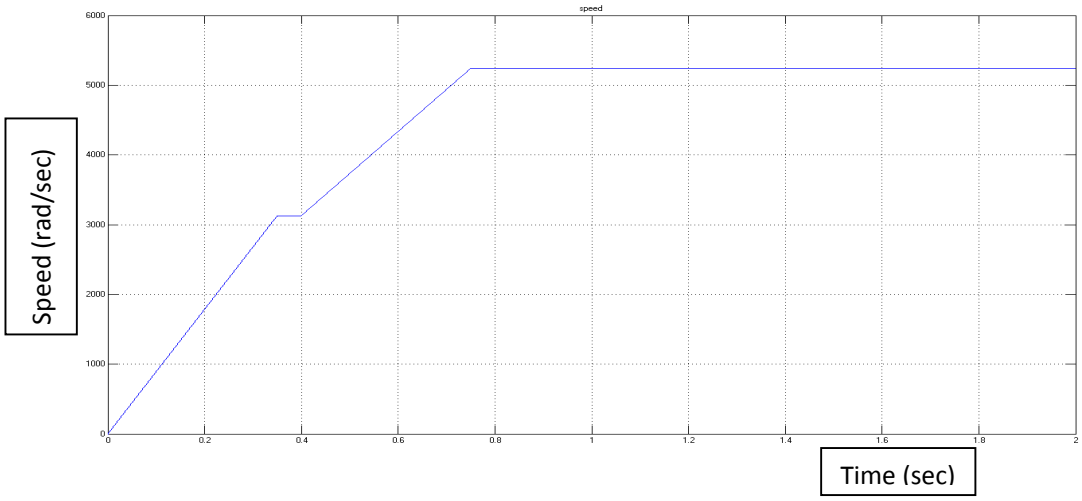

Fig. 3.16 SPEED VARIATION OF PMSM

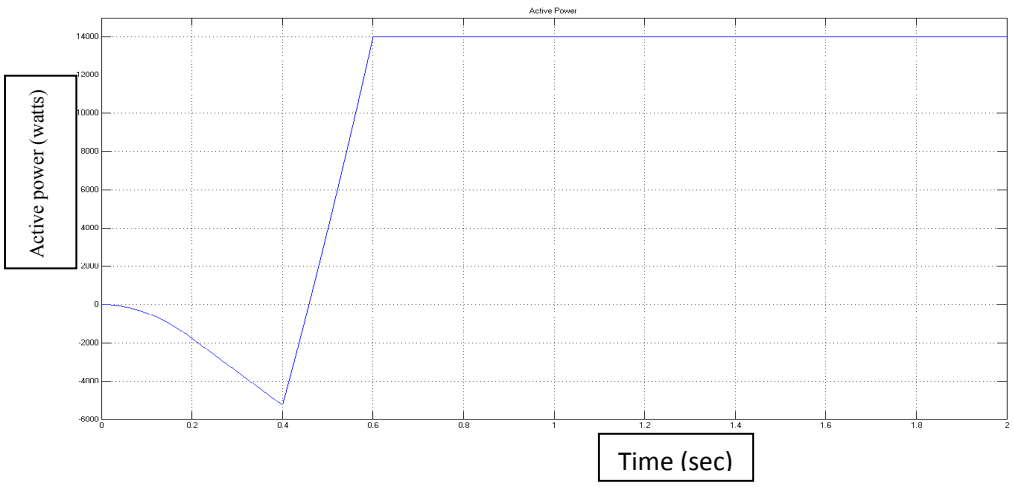

Fig.3.17 ACTIVE POWER VARIATION DURING MOTORING/GENERATING MODE AT THE GRID SIDE OF MTG

Fig 3.18 shows the Line Current of the PMSM operating in both Motoring mode and Generating mode. At the time of switching from Grid connected to Islanding operation at 1 sec, there is increase in line current of PMSM. Fig. 3.19 shows the reactive component of current injected into the grid for zero reference value of i_q.

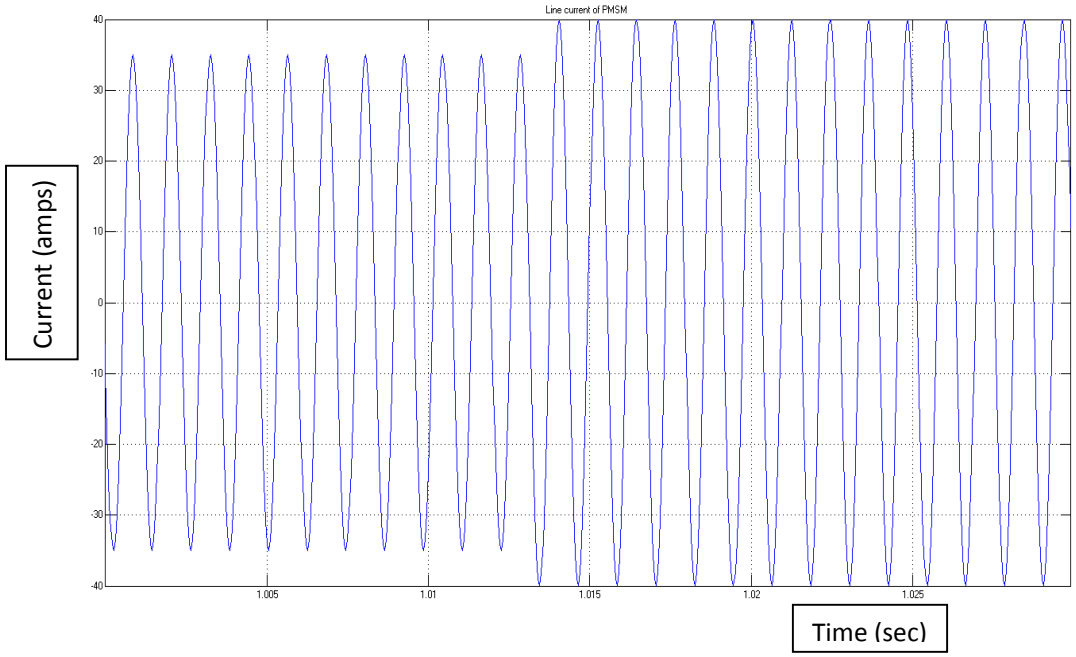

Fig. 3.18 LINE CURRENT OF PMSM

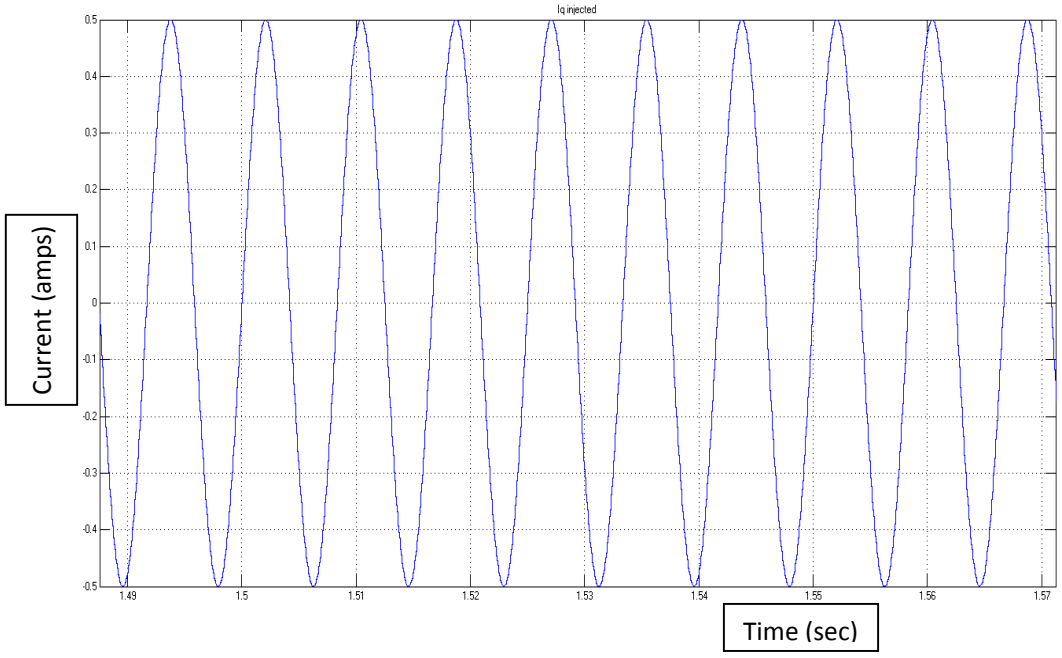

Fig. 3.19 INJECTED CURRENT I_q INTO THE GRID

Fig. 3.20 shows the DC bus voltage regulated at 760 V when the machine is operating in grid-connected mode. At the time of switching from Grid connected to Islanding operation there is dip in DC link voltage as shown in the figure.

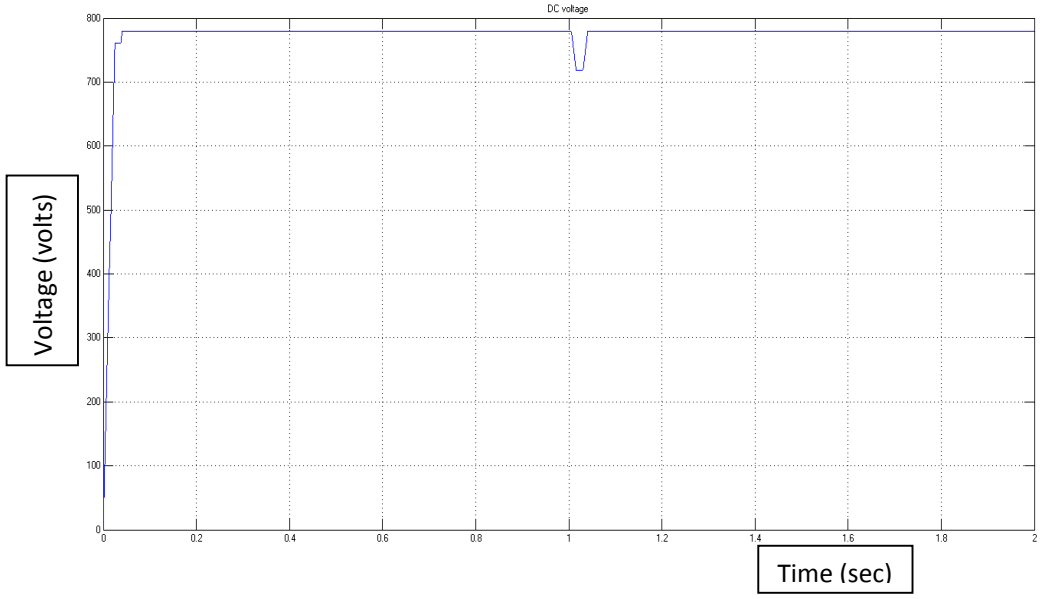

Fig.3.20 DC LINK VOLTAGE

At t=1 sec, the interface circuit breaker between MTG system and grid is opened and the voltage-frequency (Vf) control scheme for island operation is activated. Fig. 3.21 shows the line current variation of MTG system both during grid connected and islanding operations.

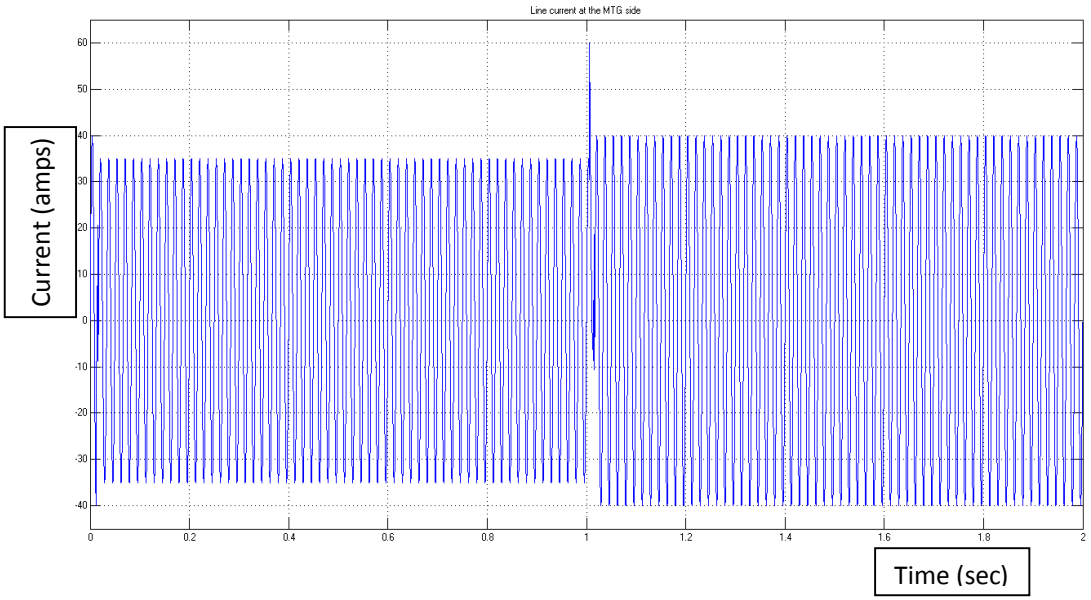

Fig.3.21 LINE CURRENT AT THE MTG SIDE

The terminal voltage at the load is shown in Fig. 3.22 when MTG system is operating at both Grid connected and Islanding mode

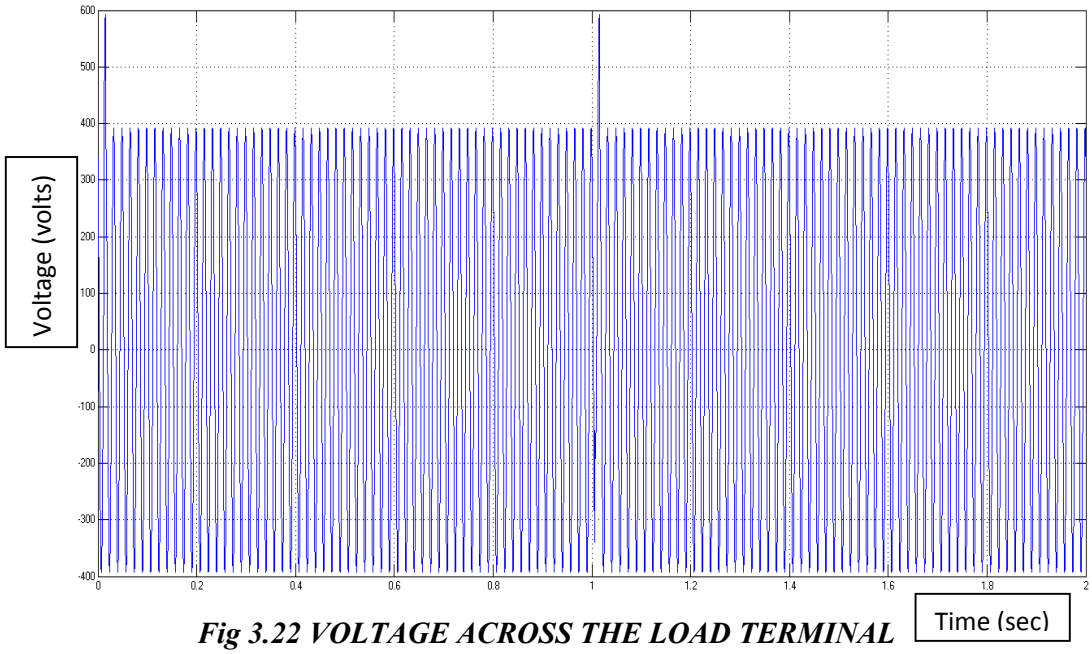

Fig 3.22 VOLTAGE ACROSS THE LOAD TERMINAL

Fig. 3.23 shows that the Load Current remains constant both during the Grid connected and Islanding mode.

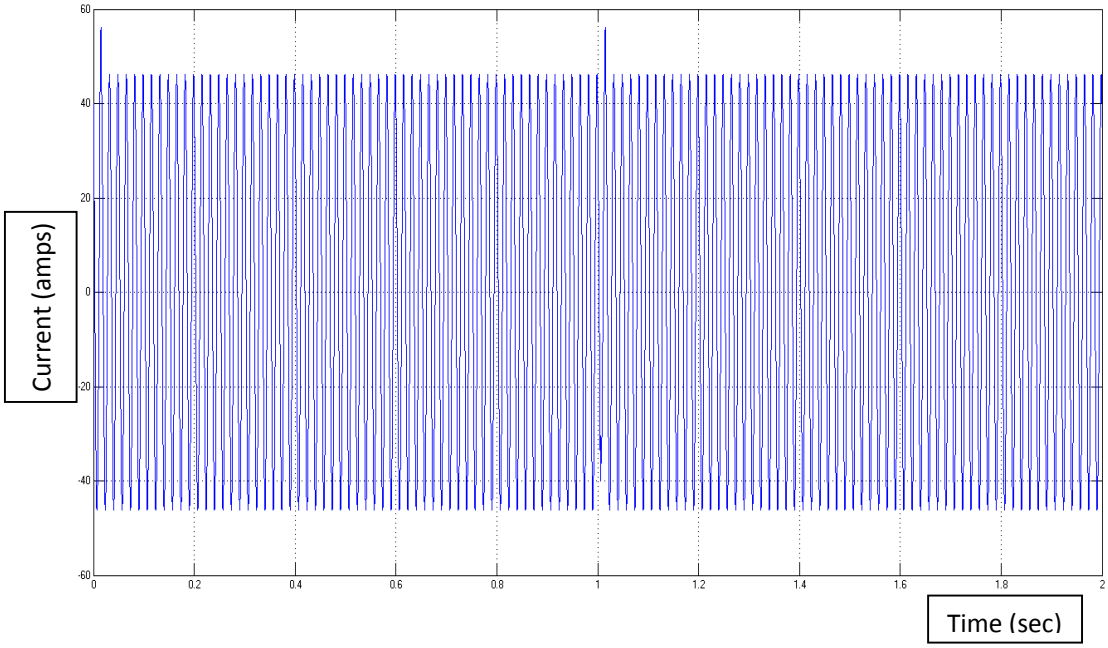

Fig.3.23 LINE CURRENT VARIATION OF THE LOAD

CHAPTER 4

MODELING AND PERFORMANCE OF FUEL CELL SYSTEM

4.1 INTRODUCTION

The fuel cells (FCs) offer the potential for lower emissions and higher efficiencies but is likely to be too expensive for many applications. The first FC unit was discovered and developed in 1839 by Sir William Grove. However, it was not practically used until the 1960's when it was utilized to supply electric power for spacecraft. Nowadays, FCs is being used in many applications because of their power quality, high efficiency, modularity, and environmental benefits. FC is an emerging small-scale power generation technology that converts hydrogen (from a fuel source) and oxygen (from air) into water and generates electricity from this electrochemical process.

A fuel cell is an electrochemical device that converts the chemical energy of the fuel (hydrogen) into electrical energy. It is centered on a chemical reaction between the fuel and the oxidant (generally oxygen) to produce electricity where water and heat are byproducts. This conversion of the fuel into energy takes place without combustion. Generally, efficiency of the fuel cells ranges from 40-60% and can be improved to 80-90% in cogeneration applications [8-10]. The waste heat produced by the lower temperature cells is undesirable since it cannot be used for any application and thus limits the efficiency of the system. The higher temperature fuel cells have higher efficiency since the heat produced can be used for heating purposes.

4.1.1 WORKING OF FUEL CELL

The structure and the functioning of a fuel cell are similar to that of a battery except that the fuel can be continuously fed into the cell. The cell consists of two electrodes, anode (negative electrode) and cathode (positive electrode) separated by an electrolyte. Fuel is fed into the anode where electrochemical oxidation takes place and the oxidant is fed into the cathode where electrochemical reduction takes place to produce electric current and water is the primary product of the cell reaction. Fig. 4.1 shows the flows of reactants in a simplified fuel cell.

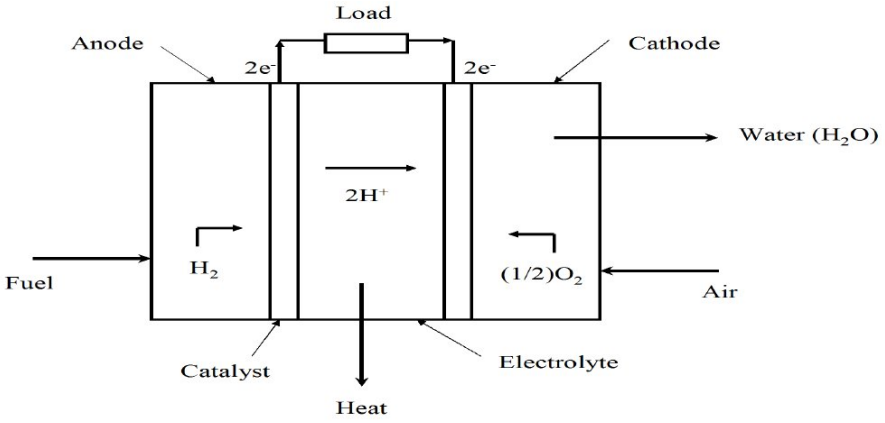

Figure 4.1 Schematic of an individual fuel cell

The hydrogen which enters the anode side is broken into hydrogen ions and electrons with the help of the catalyst. In case of lower temperature cells like the PEMFC and the PAFC, the hydrogen ions move through the electrolyte and the electrons flow through the external circuit. The oxygen which enters through the cathode side combines with these hydrogen ions and electrons to form water as shown in the above figure. As this water is removed, more ions are passed through the electrolyte to continue the reaction which results in further power production. In the SOFC, it is not the hydrogen ions which move through the electrolyte, but the oxygen radicals. In case of MCFC, carbon dioxide combines with the oxygen and electrons to form carbonate ions, which are transmitted through the electrolyte [25]. Fuel cells are classified based on the type of electrolyte used. A solid polymer membrane electrolyte is fitted between two platinum-catalyzed porous electrodes for PEM fuel cells. MCFCs have a liquid lithium-potassium or lithium-sodium based electrolyte while SOFCs employ a solid yittrastablized zirconia ceramic electrolyte. The catalyst used for SOFC and MCFC are perovsikites and nickel, respectively, the cost of which is comparatively lower than that used for PEMFC. The typical anode and cathode reactions for a hydrogen fuel cell are given by Equations (4.1) and (4.2), respectively.

$$H_2 \rightarrow 2H^+ + 2e^- \tag{4.1}$$

$$\frac{1}{2}O_2 + 2H^+ + 2e^- \rightarrow H_2O \tag{4.2}$$

An individual fuel cell produces less than a volt of electric potential. A large number of cells are stacked on top of each other and connected in series (with bipolar connects) to produce higher voltages. Figure 4.2 shows cell stacks which consists of repeating units, each comprising an anode, cathode, electrolyte and a bipolar separator plate. The number of cells depends on the desired power output [27, 28].

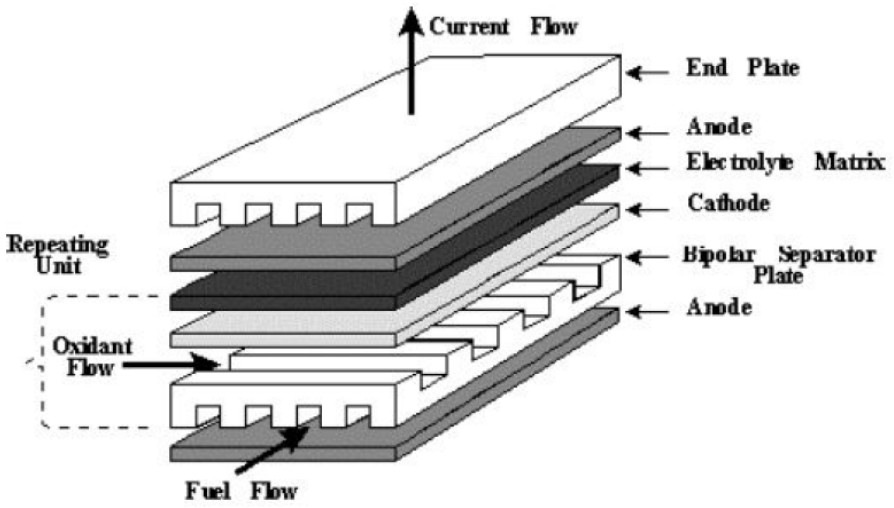

Figure 4.2 Components of a fuel cell stack

A fuel processor converts the primary fuel source (hydrocarbons) into the fuel gas (hydrogen) required by the fuel cell stack. The processor uses a catalytic reaction to break the fuel into hydrogen and separate it from the carbon based gases. Each of the fuel cell types has specific fuel requirements. Natural gas and petroleum liquids contain sulphur compounds and have to be desulphurized before they can be used as a fuel. The anode catalysts are intolerant of sulphur and it must be removed before it degrades catalyst performance. There is a risk of carbon formation in fuel cell systems which can be reduced by carrying out pre-reforming of the fuel gas before it is fed to the reformer reactor. Carbon monoxide can be used as a fuel for SOFC and MCFC because it can be internally converted to hydrogen whereas the PEMFC should be completely free from it. Carbon monoxide has high affinity for anode catalyst (especially platinum) and it prevents the flow of fuel in the PEMFC. Ammonia is a poison for all the fuel cell types due to its adverse effects on the cell life except for SOFC, where it can be internally reformed.

Lower-temperature fuel cells require an external reformer to obtain the hydrogen rich fuel, thus increasing the cost and thereby reducing the efficiency. Higher temperature fuel cells do not require an external reformer; its high temperature allows direct conversion of natural gas to hydrogen. High temperature requires stringent materials which increases the cost of the fuel cells. Hence, researchers are working to combine the benefits of the PEMFC and the PAFC to obtain intermediate temperature cells, often referred to as high temperature PEM.

4.1.2 BENEFITS AND DRAWBACKS OF FUEL CELLS

FC power plants have demonstrated better reliability and durability than other sources. As they rely on chemical instead of combustion process, FCs can run continuously for long time without breakdown due to the absence of combustion and moving parts. The main advantages of utilizing FCs include [36, 37-39]:

- **Operation at High Efficiencies**
- **Reduction of Air Pollution**
- **Fuel Flexibility**
- **Possibility of Cogeneration**
- **Modularity and Simplicity of Installation**
- **Silent Operation**
- **Suitable for the Integration with Renewable Energy Sources**

- FCs operates at **higher efficiencies** than combustion based sources since they eliminate the intermediate steps of combustors and mechanical devices used in turbines and pistons. A typical electrical efficiency of FCs lies in the range of 40% to 60%, while the utilization of both electrical and thermal power increases the overall efficiency to 70% for small units and 75% for large units [39]. Unlike conventional systems, FCs operates at high efficiencies also at partial load and in many cases the part of load efficiency is higher than the full load value. In addition, small units provide similar high efficiencies like large units due to their modularity [38].

- The emissions from FCs running on pure hydrogen are just water vapor, which could dramatically reduce greenhouse gas emission. FCs that use reformers to convert hydrocarbon fuels such as natural gas to hydrogen emit small amounts of air pollutants but still much smaller than emissions from the cleanest fuel combustion systems.

- FC system is capable of generating electricity using hydrogen extracted from a variety of sources like natural gas, ethanol, methanol, coal, and even gasoline. Also, it is possible to utilize hydrogen from renewable sources such as biomass and from wind and solar energy through electrolysis.

- In addition to the electrical energy produced in FCs, a considerable amount of useful exhaust heat is also generated as a result of the electrochemical process. In some

cases, the thermal energy produced is higher than the electrical energy. Thus, FCs are well suited for CHP operation, which contributes in increasing the unit efficiency.

- FC stack is manufactured by augmenting individual cells in parallel (to reach the required current and capacity) and in series (to obtain the suitable voltage). This advantage enables the operator to form modules with different capacities and voltages to be suitable for different purposes starting from portable units to utility applications.

- FCs are quiet sources (a 40kW FC power plant has a sound level of 68dB at a point 10 feet from the cabinet) [38]. This gives the chance to place the FC plant in the load centre near the end user, which eliminates the need for long transmission.

- FC power plants can be integrated more efficiently with renewable energy sources [31-32]. They can smooth out the oscillations occurring when using PV arrays or wind turbine and, hence, the power from these sources can be maximized without any modification in the control system. In this case, it will be possible to have significant levels of renewable power penetration. Also, the load requirements will be met more efficiently as the system reliability will be increased.

The main drawback of FCs is

- Their extremely high cost. Their production cost has to be significantly reduced to become commercially comparable with the conventional power plants. Also, more efforts and researches are required to demonstrate endurance and reliability of high temperature units.

- Fuelling fuel cells is still a problem since the production, transportation, distribution and storage of hydrogen is difficult.

- Reforming hydrocarbons via reformer to produce hydrogen is technically challenging and not clearly environmentally friendly.

- Fuel cells are in general slightly bigger than comparable batteries or engines. However, the size of the units is decreasing.

4.1.3 APPLICATIONS OF FUEL CELLS

In spite of the similarity in the operating principles, the variety of materials, operating temperatures, power densities and utilized gases expands the applications of FCs to cover most of known fields. Some of these applications are given in the following [39].

- **Portable Power**
- **Transportation**
- **Stationary Power Generation**

- Portable power refers to systems that generate power of few watts up to few hundred watts. In portable power applications, FCs would be merged to the electronic device with a small container of fuel or compressed hydrogen inserted into an inlet port. A very small blower can be used to supply air, which can also be supplied by natural convection. A new fuel container can replace the old one when the fuel is completely depleted [39]. Unlike batteries, recharging would not be necessary and also new fuel container would be lighter and less expensive. Examples include power for portable electronic devices such as laptops and power for soldiers deployed in the field.

- FCs are expected to thrive in the field of vehicle application as they represent a clean energy technology [37]. Many attempts are directed to advance the FC technology to produce a power source at a cost and volume that are competitive with the existing internal combustion engine. PEMFC has attained a special attention due to its fast acceleration rate and high power densities, which reduces the required accommodation place. Most of the technical objectives are directed to decrease the production cost and to solve the fuel supply problems [36].

- FCs is promising sources for stationary applications including distributed power generation for utilities, backup power generation industry and cogeneration applications [36, 37]. FCs is advantageous due to their high efficiency, modularity, and low environmental impacts. Also, they can be beneficial and attractive sources in remote areas to solve many problems in the congested distributed systems. In these cases, it would be more economical to add a new decentralized source near the load than upgrading the utility grid [38, 36].

4.2 TYPES OF FUEL CELLS

The general classifications of fuel cells are based on the type of electrolyte used. There are many types of fuel cell such as alkaline fuel cells (AFCs), phosphoric acid fuel cells (PAFCs), proton exchange membrane fuel cells (PEMFCs), molten carbonate fuel cells (MCFCs) and solid oxide fuel cells (SOFCs). Fuel cells can further be classified based on operating temperature [28]. Various characteristics are summarized [8-10].

Table 3 A basic summary of various Fuel cells characteristics.

Criteria	AFCS	PEMFC	PAFC	MCFC	SOFC
Operating Temp.	80-100 ˚C	50-100 ˚C	~200 ˚C	600-700 ˚C	500-1000 ˚C
Operating Pressure	1-5 atm	1-5 atm	1-8 atm	1-3 atm	1-13 atm
Size Range	50-100 kW	3-250 kW	100-200 kW	250 kW-10 MW	1 kW-10 MW
Efficiency	35-60 %	35-40 %	35-40 %	50-55 %	45-50 %
Fuel	H_2	H_2	H_2	H_2, CO, CH_4	H_2, CO, CH_4, NH_3
Charge Carrier	H^+	H^+	H^+	CO_3^{2-}	O^{2-}
Construction Material	Graphite Carbon	Graphite Carbon	Graphite Carbon	Ni and Stainless Steel	Ceramics and Metals
Cooling Medium	Water	Water	Boiling Water	Excess air	Excess air

According to the type of electrolyte, the different types of fuel cells are discussed below as :

Alkali fuel cells

The alkali fuel cell (AFC) was one of the first modern FCs to be developed, beginning in 1960 when it is used by NASA on space missions [36]. A liquid solution of potassium hydroxide is used in AFC as an electrolyte. Generally, the slowness of FCs is defined by the cathode reaction because it takes more time to react than the anode reaction. AFC is characterized by a faster cathode reaction than other types of FCs, which enhances its overall performance and speeds up its electrical response. The lower

operating temperature (80-100°C) gives a fast start advantage for this type of FCs, which can achieve efficiencies up to 60%.

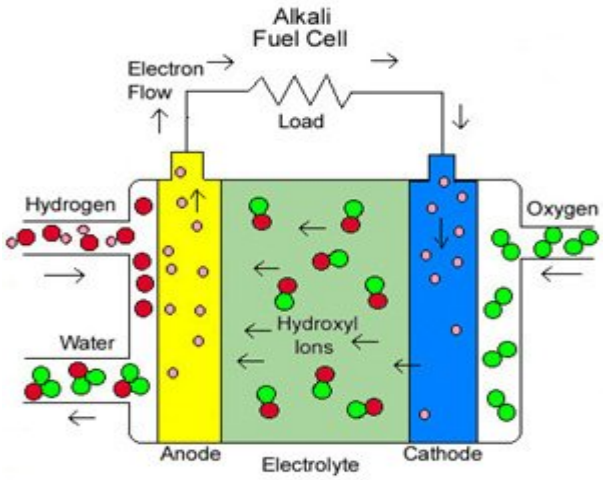

Fig. 4.3 Alkali fuel cell (AFC)

Molten Carbonate fuel cells:

Many of the disadvantages related to low temperature FCs can be alleviated by increasing the operating temperature. The molten carbonate fuel cell (MCFC) is a promising high temperature FC (operates at 650 °C), which uses molten alkali carbonate mixture as an electrolyte (usually consists of lithium carbonate and potassium carbonate). At these high temperatures, precious metal catalysts are not required for the FC reactions, rather, the cell reactions occur with nickel catalysts. In addition, the heat available from the stack is high enough for cogeneration applications.

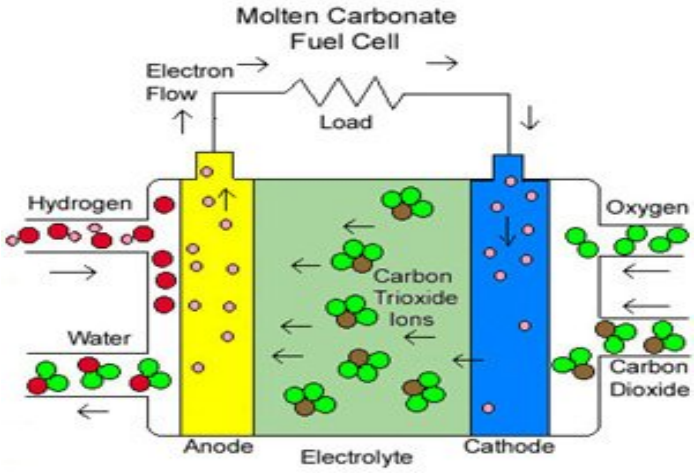

Fig. 4.4 Molten Carbonate fuel cell (MCFC)

Phosphoric Acid fuel cells:

The phosphoric acid fuel cell (PAFC) has been under development for more than 20 years and was the first commercial FC. This caused a significant reduction in the cost and remark able increase in the efficiency. It utilizes a liquid phosphoric acid as an electrolyte with an operating temperature of 200°C. This temperature is high enough to facilitate the recovery of heat for water and space heating. It prevents also the water, which is produced as a sub product, from dissolving in the liquid electrolyte [39]. Higher operating temperatures are not possible since the phosphoric acid begins to decompose at 210 °C. PAFC generates electricity at more than 40% efficiency, which can be significantly increased with the use of the produced steam in cogeneration.

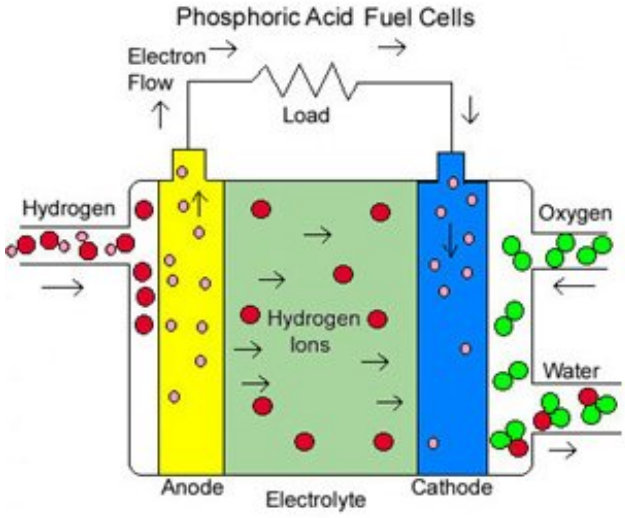

Fig. 4.5 Phosphoric Acid fuel cell (PAFC)

Proton Exchange Membrane:

The proton exchange membrane fuel cell (PEMFC) has gained a lot of attention in the last few years as one of the most promising FC types [37]. It uses a solid organic polymer polyperflourosulfonic acid as an electrolyte. The solid electrolyte in PEMFCs has a very high resistance to gas crossover, and its membrane, which is made of Teflon like material, represents an excellent conductor of protons and an insulator of electrons [39]. The other benefits of utilizing a solid electrolyte include the lower corrosion and the absence of the liquid management.

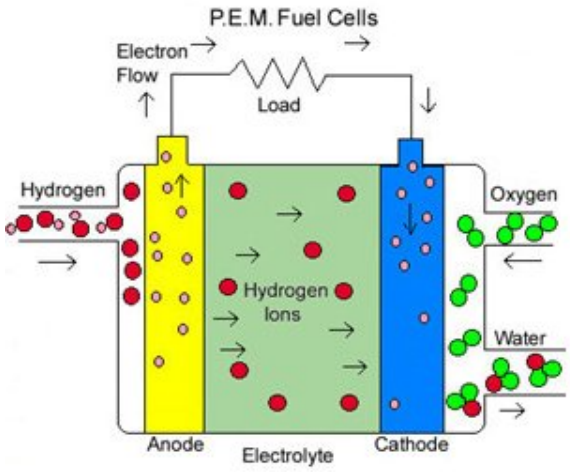

Fig. 4.6 Proton Exchange Membrane (PEM)

Solid Oxide fuel cells:

The solid oxide fuel cell (SOFC) has the longest continuous development period, starting in the late 1950s [9, 10, 38]. Solid Oxide fuel cells (SOFC) use a hard, ceramic compound of metal (like calcium or zirconium) oxides (chemically, O_2) as electrolyte, allowing the operating temperature to reach 1000°C, which is the highest temperature of all FC systems [38, 39]. The solid ceramic material represents an excellent insulator for negatively charged ions at high temperatures. Like MCFC, SOFC can use carbon dioxide as well as hydrogen as its direct fuel but without any requirements for CO_2 at the cathode. The high temperature helps to increase the unit efficiency and gives the SOFC the ability to use a wide variety of less expensive catalysts than the low temperature FCs.

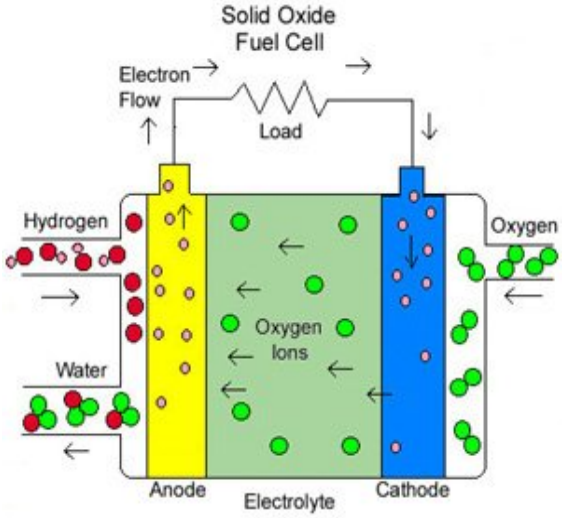

Fig. 4.7 Solid Oxide fuel cell (SOFC)

The configuration of SOFC is also simpler due to possibility of internal reforming. The high operating temperature gives also the facility for developing cogeneration systems or using hybrid configurations, where SOFC is augmented with gas turbines and/or steam units [38]. Furthermore, the solid electrolyte eliminates the corrosion and management problems, which regularly happen with liquid electrolytes.

On the other hand, the high operating temperature has some disadvantages since it speeds up the breakdown of the cell components, which shortens the life of many parts of the unit [39]. SOFCs are being considered mainly for medium and large scale power generation. However, efforts succeeded to develop SOFC for small applications. Since the electrolyte is solid, the cell can be formed in a variety of configurations such as tubular and planar types.

4.3 MODEL OF FUEL CELL SYSTEM

Fuel cells produce DC power, water and heat from the combination of hydrogen produced from the fuel and oxygen from the air. In procedures where CO and CH_4 react in the cell to produce hydrogen, CO_2 is also a co-product. Reactions in fuel cells depend substantially on the temperature and pressure inside the cell. A system must be built around the fuel cell to supply air and clean fuel, convert the energy to a more usable form such as grid quality ac power, and remove the depleted reactants and heat that are produced by the reactions in the cells. Fig. 4.8 shows the basic structure of a fuel cell power plant.

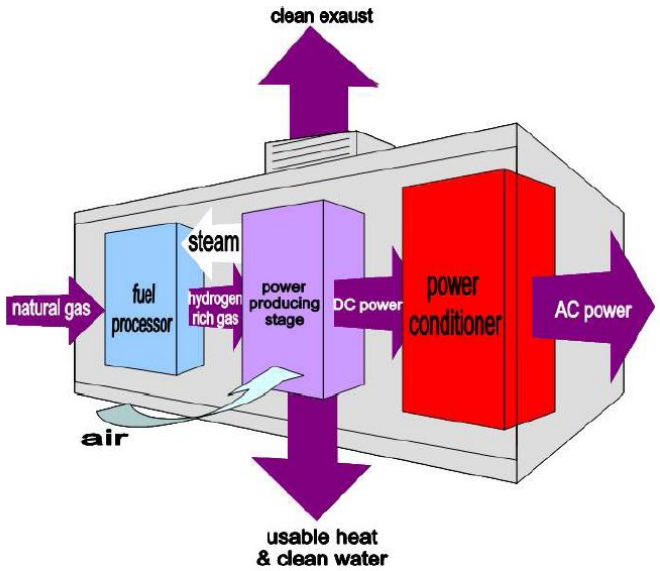

Fig. 4.8 Block diagram of a fuel cell system

First stage of a fuel cell power system plant is a fuel processing unit where a conventional fuel (natural gas, methanol, coil, naphtha, or other gaseous hydrocarbon) is purified into a gas containing hydrogen. The following stage converts chemical energy to DC electricity using the stacks of individual fuel cells. Number of stacks used in the power producing section unit depends on the specific power application. Finally, power conditioner converts DC power generated by the fuel cell stacks into the regulated AC or DC power suitable for customer usage.

4.3.1 MODEL OF SOFC

SOFCs have fuel-flexibility, the input to the anode can be hydrogen, carbon monoxide or methane. Hydrogen or carbon monoxide may enter the anode. At the cathode, electrochemical reduction takes place to obtain oxide ions. These ions pass through the electrolyte layer to the anode where hydrogen is oxidized to obtain water. In case of carbon monoxide, it is oxidized to carbon dioxide.

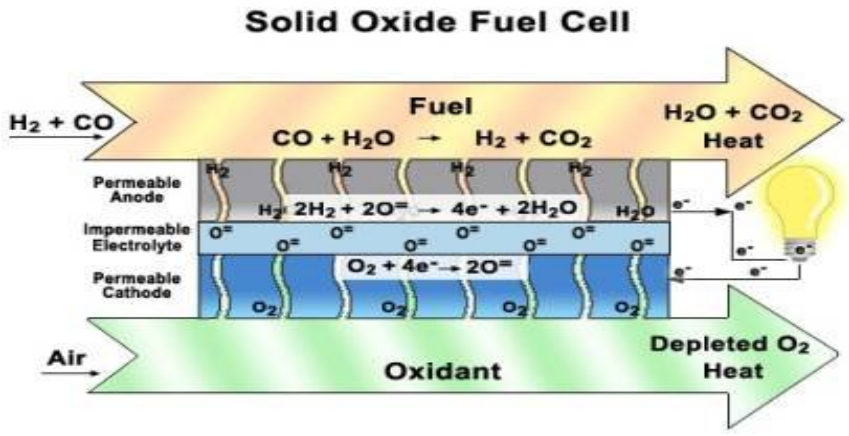

Figure 4.9 Operating concept of a SOFC

The modeling of SOFC is based on the following assumptions

- The fuel cell temperature is assumed to be constant.
- The fuel cell gasses are ideal.
- Nernst's equation applicable.

A simulation model is developed for the SOFC in MATLAB based on the dynamic SOFC stack. Considering ohmic losses of the stack, the expression of total stack voltage can be written as

$$V_{fc} = N_o\left(E_o + \frac{RT}{2F}\left(\ln\frac{P_{H_2}P_{o_2}^{\ 0.5}}{P_{H_2O}}\right)\right) - rI_{fc} \tag{4.3}$$

V_{fc} – Operating dc voltage (V)

E_o – Standard reversible cell potential (V)

P – Partial pressure of species i (Pa)

r – Internal resistance of stack (S)

I – Stack current (A)

N0 – Number of cells in stack

R – Universal gas constant (J/ mol K)

T – Stack temperature (K)

F – Faraday's constant (C/mol)

The output voltage of the stack is given by the Nernst equation. The ohmic loss of the stack is because of the resistance of the electrodes and to the resistance of the flow of oxygen ions through the electrolyte. Partial pressure of hydrogen, oxygen and water are given in Equations (4.4), (4.5) and (4.6). The slow dynamics of the fuel cell current is represented by Equation (4.7).

$$P_{H_2} = \left(\frac{\frac{1}{KH_2}}{1+\tau_{H_2}S}\right)\left(qH_2 - 2K_rI\right) \tag{4.4}$$

$$P_{O_2} = \left(\frac{\frac{1}{KO_2}}{1+\tau_{O_2}S}\right)\left(qO_2 - 2K_rI\right) \tag{4.5}$$

$$P_{H_2O} = \left(\frac{\frac{1}{KH_2O}}{1+\tau_{H_2}OS}\right)\left(2K_rI\right) \tag{4.6}$$

$$I = \left(\frac{I_{ref}}{1+\tau_eS}\right) \tag{4.7}$$

I_{ref} is the reference current which is given by Equation (4.8). Fuel and oxygen flow are given by Equations (4.9) and (4.10).

$$I_{ref} = \left(\frac{P_{ref}}{V_{fc}} \right) \tag{4.8}$$

$$qH_2^r = 2K_r I \tag{4.9}$$

$$qO_2^r = \frac{qH_2}{rHO} \tag{4.10}$$

The power output of the fuel cell system is the product of stack current and voltage. The block diagram represents SOFC dynamic model is shown in the Figure 4.10.

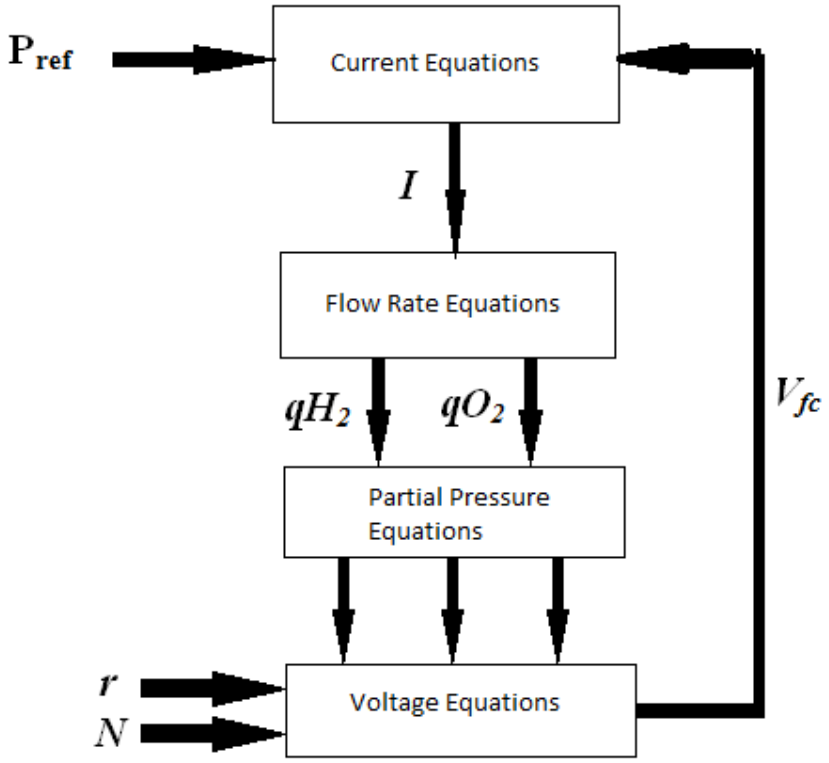

Figure 4.10 Block diagram for dynamic model of SOFC

By taking the dynamic model equations of the SOFC and relative data (Table 4.) and simulated it in MATLAB/SIMULINK which was shown in Figure 4.11

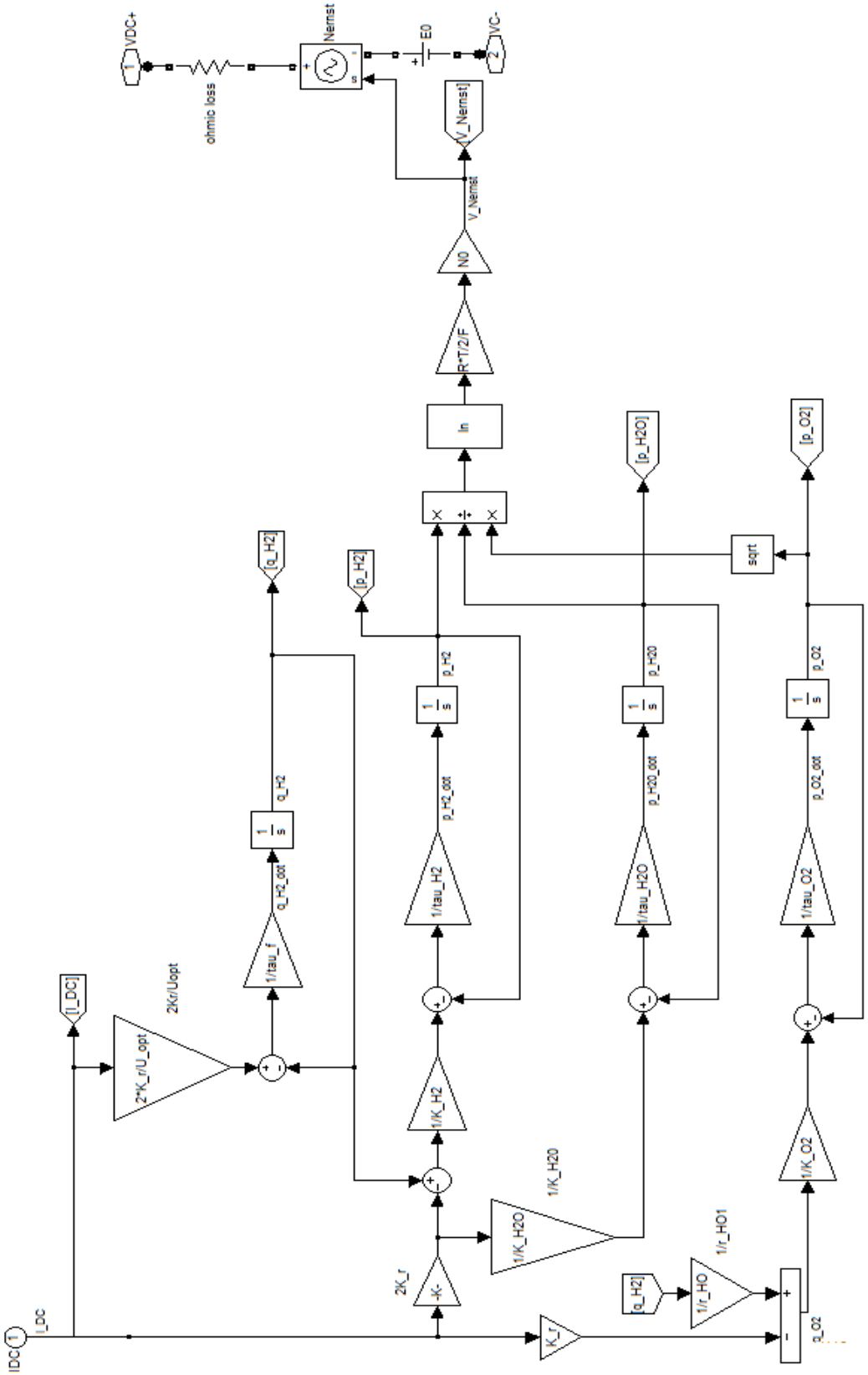

Figure 4.11 Simulink circuit of SOFC

Table 4 Parameters in SOFC model [10], [25], & [31]

Symbol	Representation	Value
T	Absolute temperature	1273 K
F	Faraday's constant	96487 C/mol
R	Universal gas constant	8314 J/(kmol K)
E°	Standard reversible cell potential	1.18 V
N	Number of cells in stack	384
K_r	Constant, K_r =N/4F	0.996×10^{-6} kmol/(s A)
Umax	Maximum fuel utilization	0.9
Umin	Minimum fuel utilization	0.8
U_{opt}	Optimum fuel utilization	0.85
KH_2	Valve molar constant for Hydrogen	8.43×10^{-4} kmol/(s atm)
KO_2	Valve molar constant for Oxygen	2.81×10^{-4} kmol/(s atm)
KH_2O	Valve molar constant for Water	2.52×10^{-3} kmol/(s atm)
τ_{H_2}	Response time for Hydrogen flow	26.1 s
τ_{H_2O}	Response time for Water flow	78.3 s
τ_{O_2}	Response time for Oxygen flow	2.91 s
R	Ohmic loss	0.126 Ω
T_e	Electrical response time	0.8 s
T_f	Fuel processor response time	5 s
r_{HO}	Ratio of hydrogen to oxygen	1.145
BASE MVA	Base M V A	100

4.3.2 MODEL OF POWER CONDITIONING UNIT

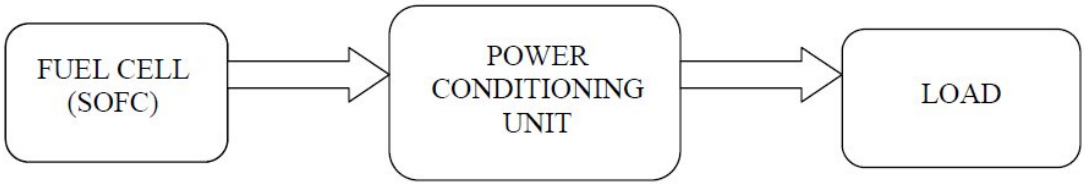

Fig 4.12: Power Conditioning Unit

The power conditioning system is shown in Fig. 4.12. The power conditioning system provides regulated dc or ac power appropriate for the application. It is the major component of an FC system. The output of the FC is an unregulated dc voltage and it needs to be conditioned in order to be of practical use. The power conditioner section converts the raw power into useable power for different applications. The power conditioning unit also controls electricity's frequency and maintains harmonics to an acceptable level. The purpose of conditioners is to adapt the electrical current from FC to suit the electrical needs of the application [27].

The general configuration of the system will be the FC followed by a boost converter followed by an inverter. In general, the load for the boost stage is a filter and the inverter system (for stand-alone purpose a purely resistive and a reactive load might be considered). The boost converters for the FC will be operated in the voltage control mode. The boost converter is ideally suited for interfacing the inverter system with the FC [29-31].

Based on the load conditions, the boost stage can be commanded to draw a specific amount of current from the FC with a ripple well defined by the frequency, size of the inductor, and duty ratio. Similarly, the inverter is used for the interfacing of the FC system to the load to provide the load with voltage/current with proper frequency phase and magnitude where the input for the inverter comes from the boost converter stage and the inverter (with the filter) becomes the load for the boost converter. The power conditioner is also used for the grid connection of the FC. An electrical power-generating system that uses FC as the primary source of electricity generation and is intended to operate synchronously, and in parallel with the electric utility network is a grid-connected FC system [29-31].

4.3.2.1 DC-DC CONVERTER CONTROL:

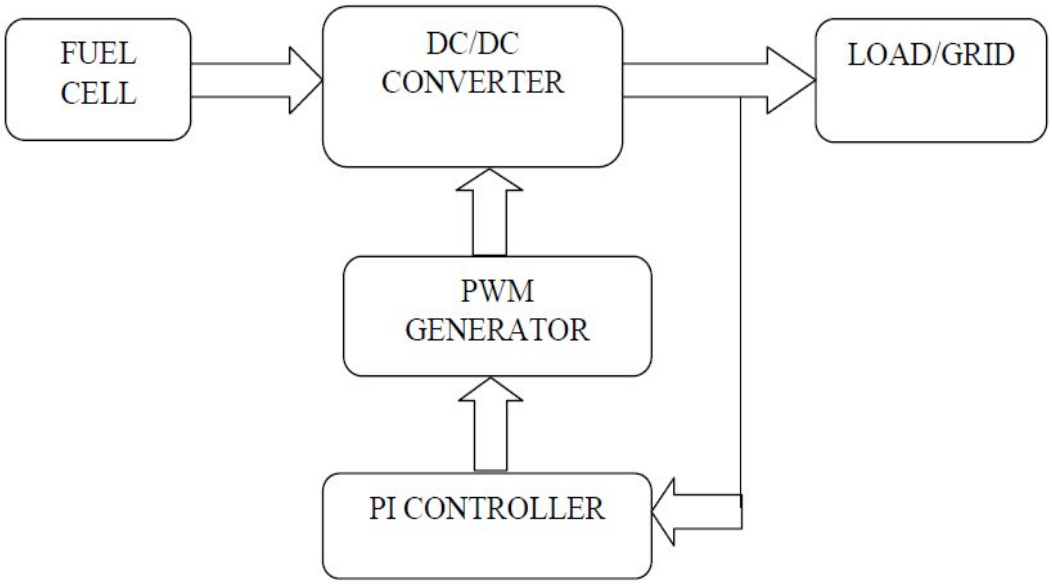

Fig 4.13 DC/DC Converter Control loop

The DC-DC converter control scheme is shown in Fig. 4.13. The output voltage of FC at the series of the stacks is uncontrolled dc voltage which fluctuates with load variations. This raw voltage, which is unregulated and uncontrolled, is regulated to an average value with help of dc/dc converter. The controlled voltage thus obtained is fed to the dc/ac inverter after it is filtered. The power obtained from this inverter is added to the grid. This system can be used as a standalone after the dc/dc converter stage if dc power is needed or after the dc/ac stage if ac power is needed [27].

This unregulated voltage has to be adjusted to a constant average value (regulated dc voltage) by adjusting the duty ratio to the required value. The voltage is boosted depending upon the duty ratio. The duty ratio of the boost converter is adjusted with the help of a PI controller The duty ratio is set at a particular value for the converter to provide desired average value of voltage at the output, and any fluctuation in the FC voltage due to change in fuel flow, in the load or in the characteristics of FC due to the chemistry involved takes the output voltage away from the desired average value of the voltage [29-31].

The PI controller changes the duty ratio properly to get the desired average value. The duty ratio of the converter is changed by changing the pulses fed to the switch in the dc/dc converter circuit by the PWM generator [39].

MODELL OF DC/DC CONVERTER

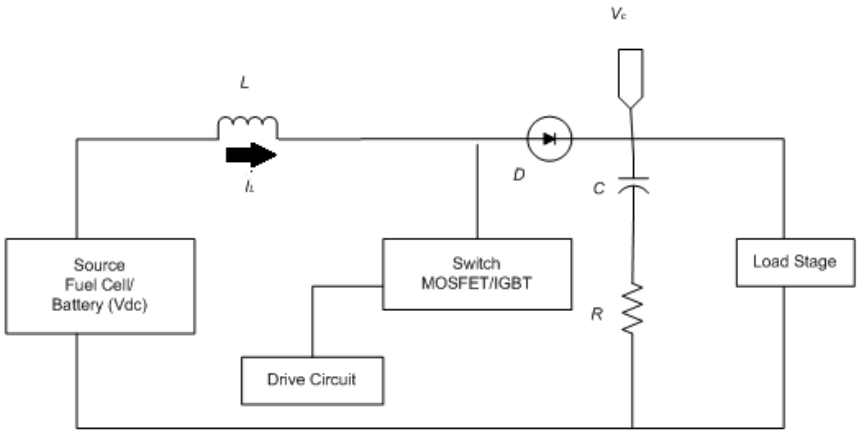

Fig 4.14 Circuit Diagram of DC/DC Converter

$$P_{in} = V_i * I_i \tag{4.11}$$

$$I_i = I_L \tag{4.12}$$

$$D = 1 - \frac{V_o}{V_i} \tag{4.13}$$

For Continuous Conduction the designed values of L, C, R is

$$R = \frac{V_o}{I_o} \tag{4.14}$$

$$L = \frac{(V_i * D)}{(f * \Delta V_C)} \tag{4.15}$$

$$C = \frac{(V_O * D)}{(f * R * \Delta V_C)} \tag{4.16}$$

SIMULATION MODEL OF DC/DC CONVERTER

The DC/DC converter boosts the low unregulated voltage to a desired regulated voltage. The input for the DC/DC converter is the fuel cell voltage and output of the DC/DC converter is connected to the inverter circuit which was shown in Figure 4.15

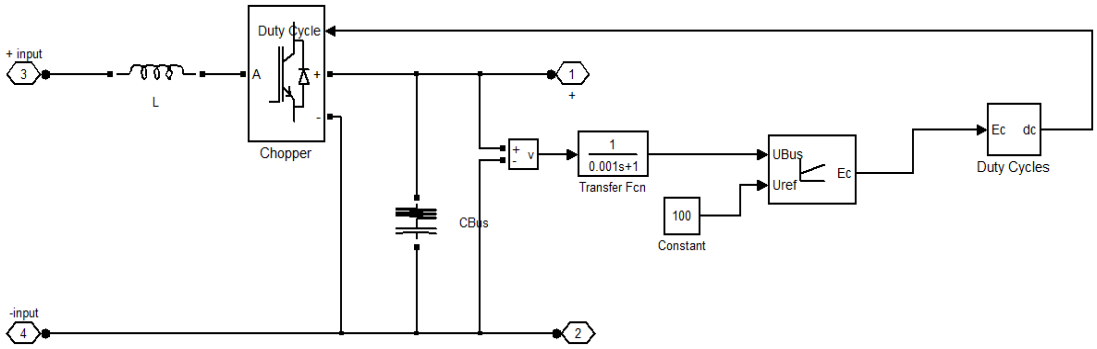

Fig 4.15 Simulink model of DC/DC Converter

4.3.2.2 DC-AC CONVERTER (INVERTER) CONTROL:

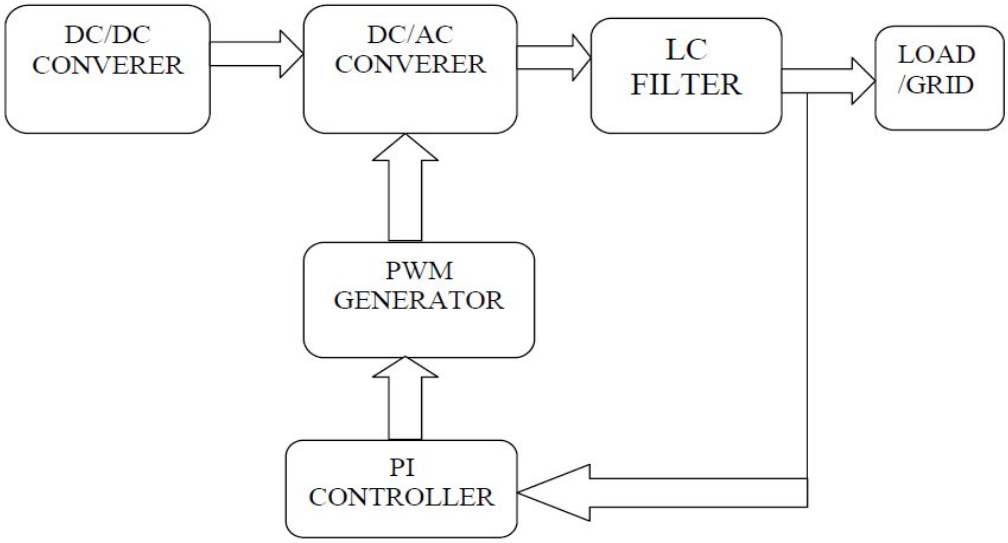

Fig 4.16 DC/AC Converter Loop

Inverters are devices that change the dc electricity produced by FC into ac electricity. Utility – interactive inverters are used in systems connected to a utility power line. The inverters produce ac electricity in synchronization with the power line, and of a quality acceptable to the utility company once the control strategy is implemented [27].

The inverter output voltage (i.e. load voltage) will be compared every time with the ref voltage. The change in the output (due to change in the load) and grid voltage is given as inputs to the PI controller, and the output of the PI controller is given to the PWM generator and this generator will generate 6 pulses [29-31].

These pulses will be given to the switches of the inverter which will change the duty ratio of the inverter. Due to this change in duty ratio the output voltage will be maintained constant during the loading conditions [39].

4.4 SIMULATION OF FUEL CELL SYSTEM

The complete simulated model of fuel cell system is shown in Figure 4.17. It shows a solid oxide fuel cell delivering dc voltage. The power conditioning unit contains dc to dc converter unit present within the Fuel cell system. The dc voltage from fuel cell system is fed to a dc capacitor to obtain constant dc voltage. This voltage is then fed to an inverter to convert dc to ac voltage. The gate pulse generation for inverter is made through hysteresis control as shown in the same figure. The ac voltage obtained from inverter contains harmonics which needs to be filtered. So, ac voltage waveform is fed to a filter system having inductor in series and capacitor in parallel. Then, the voltage is stepped up to account for the losses incurred. Also, to keep filtered ac voltage constant, it's made to pass through a smoothing reactor. The, resultant constant filtered ac voltage is then given to an infinite bus.

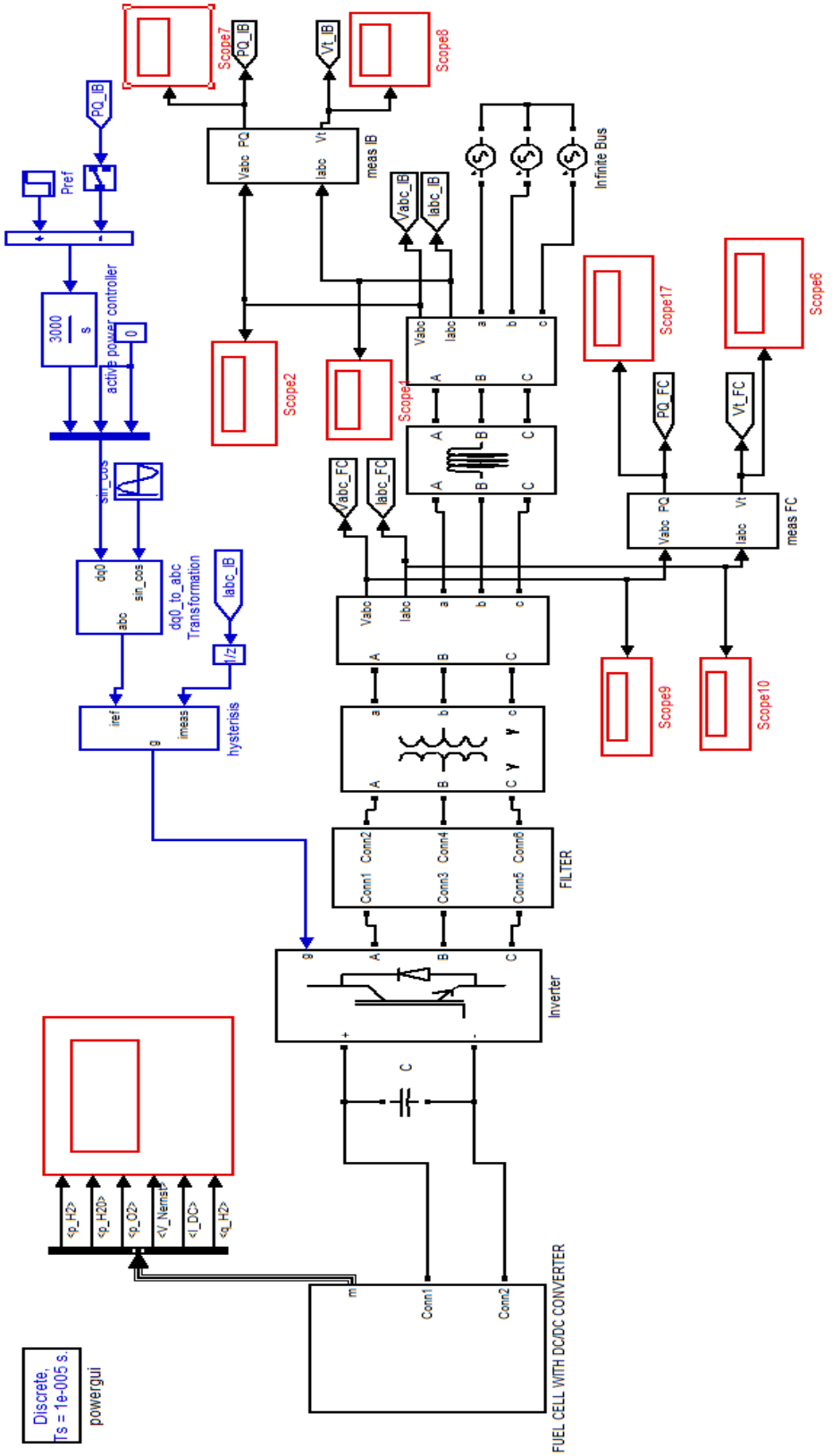

Fig. 4.17 SIMULINK MODEL OF FUEL CELL SYSTEM

4.5 RESULTS AND DISCUSSIONS

The simulink model of fuel cell system is shown in Fig. 4.17. The output of fuel cell is connected to an infinite bus through power electronic based conditioning devices various parameters are as follows.

During the simulation run, the partial pressure output characteristics of Hydrogen fuel (H_2), oxygen (O_2) and water (H_2O) of solid oxide fuel cell are shown in Fig. 4.18. The hydrogen and oxygen pressure increases initially up to 0.4 sec and then continuously decreases. The water pressure decreases up to 0.4 sec and then increases linearly. Initially hydrogen (H_2) flows into the electrolyte so the hydrogen pressure increases from 0.049 to 0.051 (mol/sec) in 0.4 sec time. After that it attains the value as 0.4 (mol/sec) at 2 sec. with the flow of hydrogen (H_2) in electrolyte, the oxygen (O_2) pressure also increases initially to 0.0515 (mol/sec) from 0.049 (mol/sec) in 0.4 sec thereafter the oxygen pressure decreases to 0.0399 (mol/sec) in 2 sec.

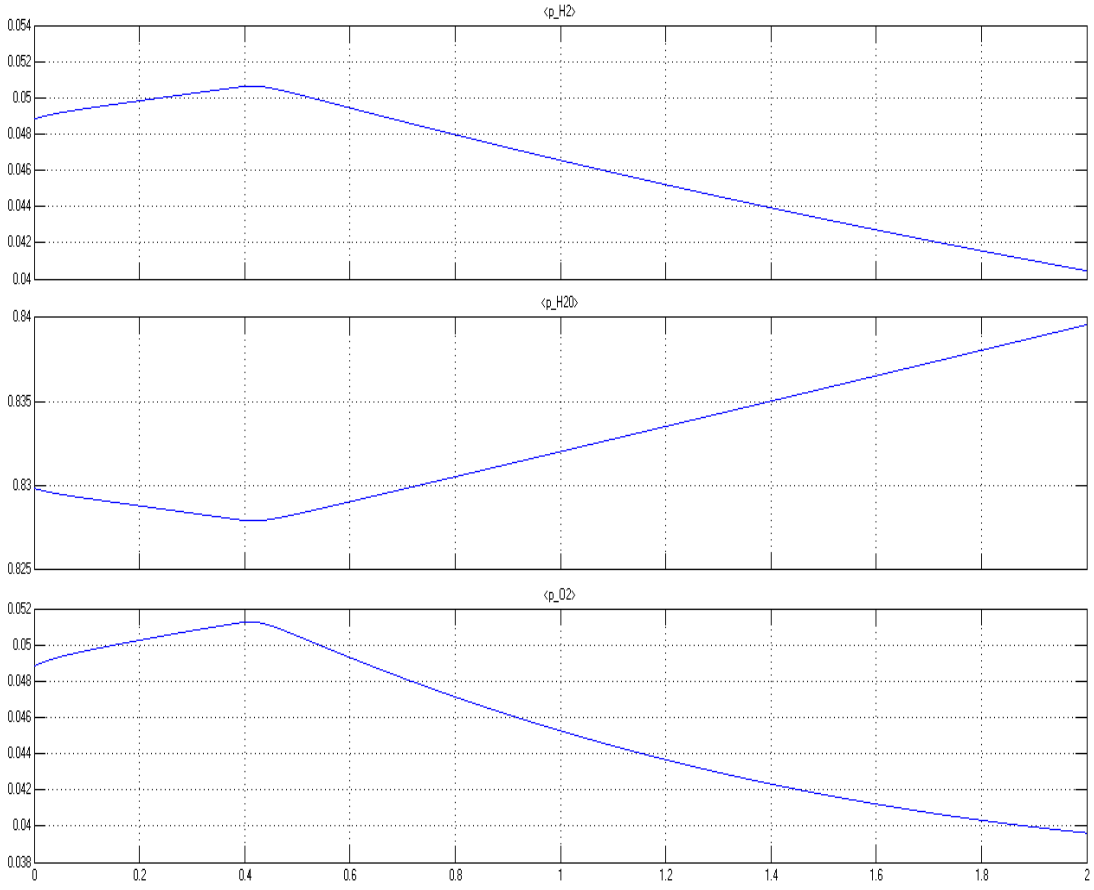

Fig. 4.18 Output of Solid Oxide Fuel Cell

Fig. 4.19 shows the variation in operating DC voltage and current of Fuel Cell. Fig. 4.20 gives the Real and Reactive power variation at Fuel cell and Infinite bus connected as load. It has been observed that the reactive power at Infinite bus is zero. Real power obtains 1 pu in 0.57 sec at fuel cell and infinite bus.

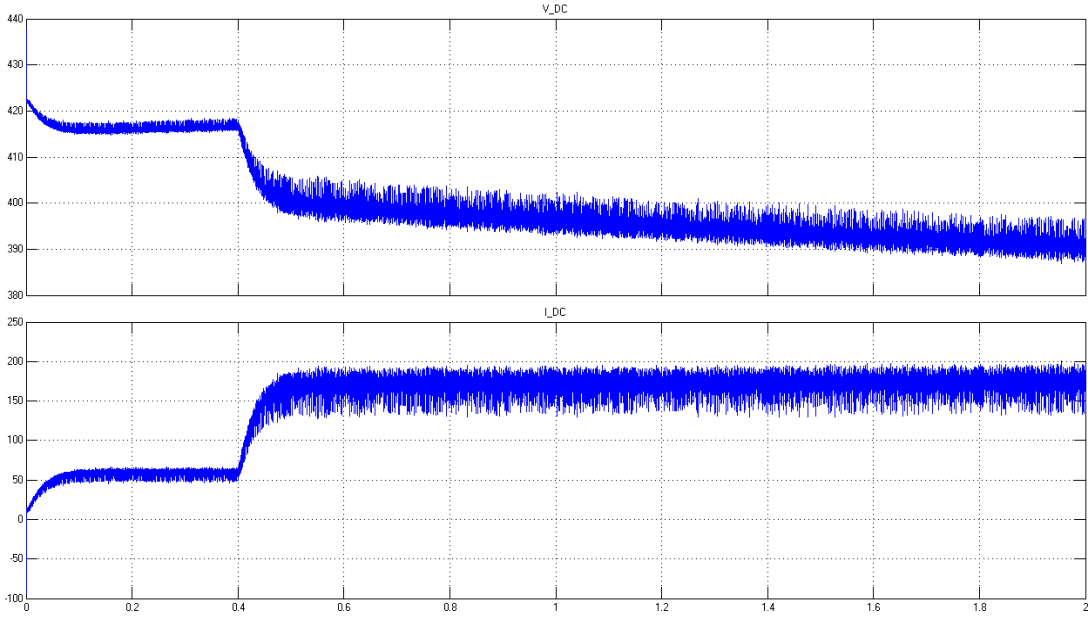

Fig. 4.19 Operating DC voltage and current of Solid Oxide Fuel Cell

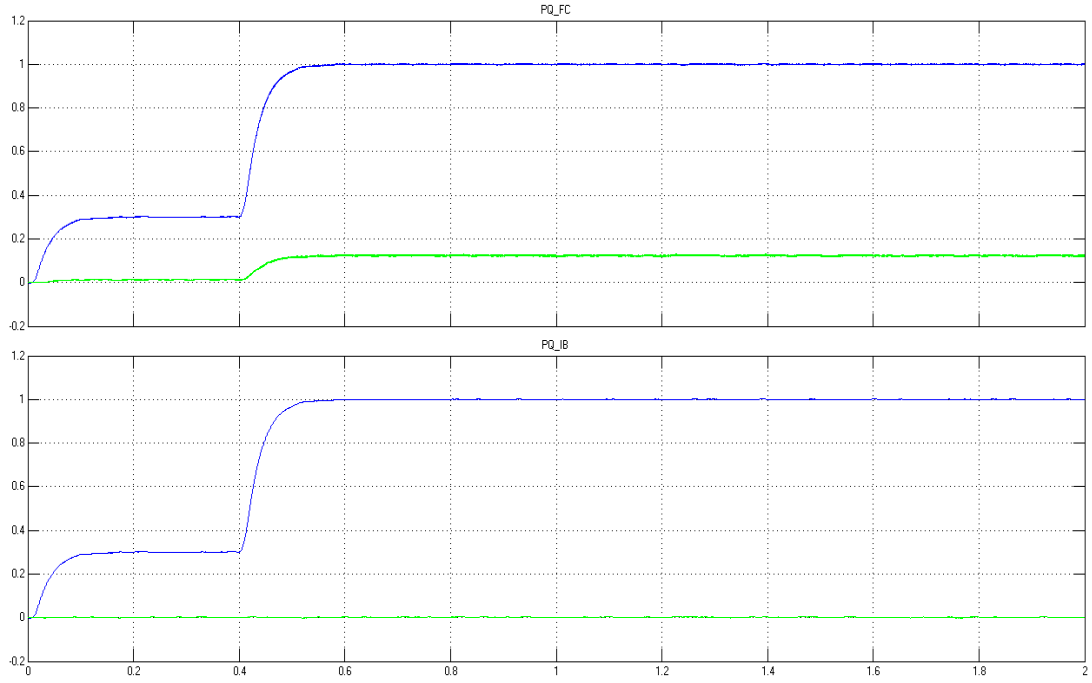

Fig. 4.20 Real and Reactive power of Fuel cell and Infinite Bus

Fig. 4.21 shows the voltage at Infinite bus and at Fuel cell. The voltage is passed through smoothing reactor before it reaches the Infinite bus. Voltage at infinite bus obtains 1 pu in 0.01 sec and it remains constant throughout.

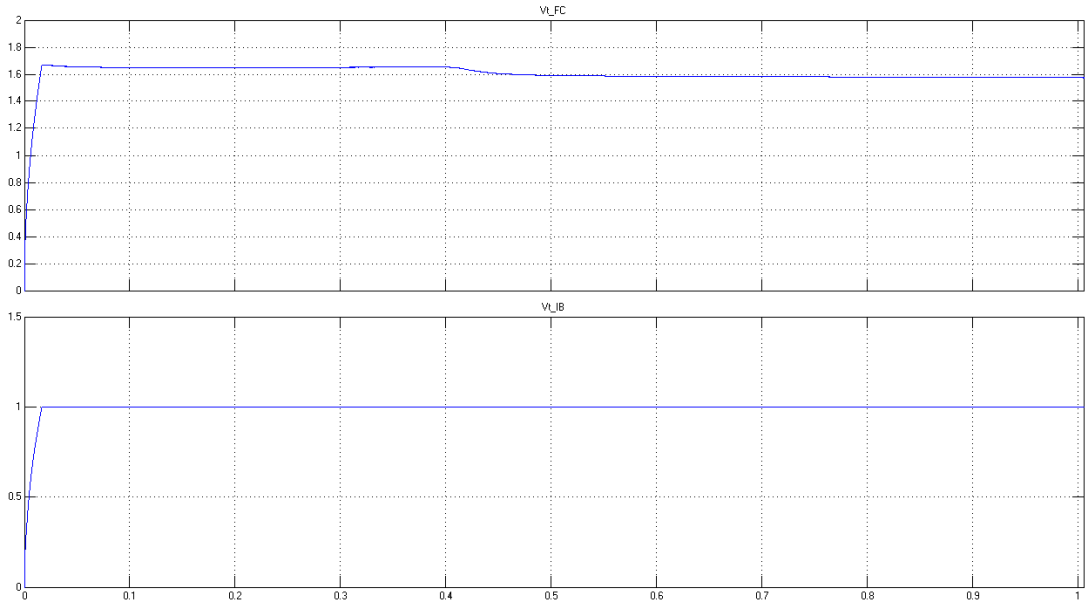

Fig. 4.21 Voltage at Fuel cell and Infinite Bus

Fig. 4.22 shows the voltage at the fuel cell (i.e before connecting to smoothing reactor) and at the Infinite bus (i.e after connecting to smoothing reactor). The current wave form at the Infinite bus is also given in the figure.

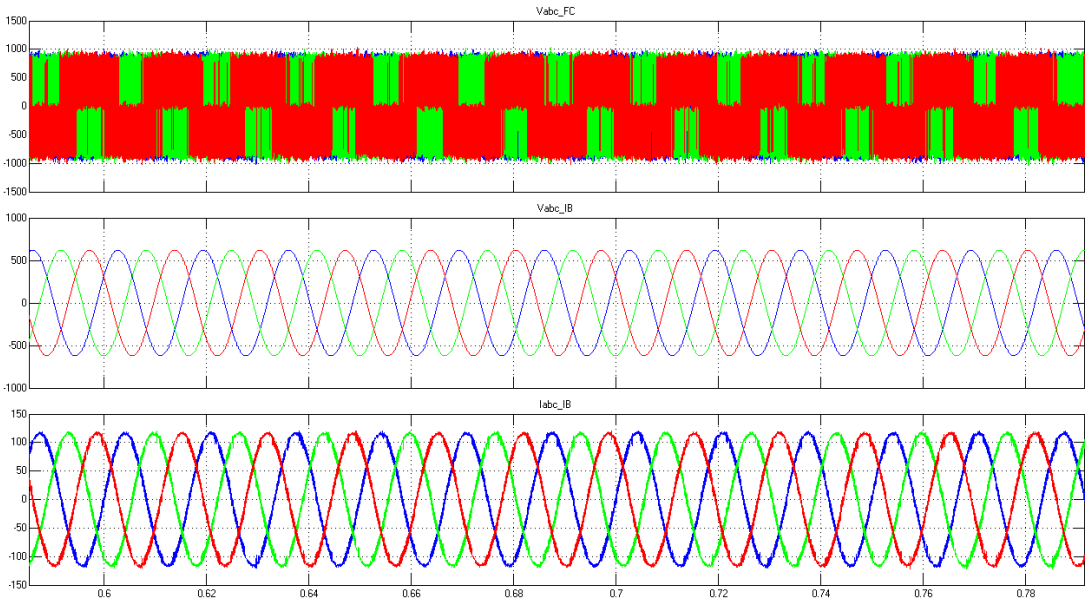

Fig. 4.22 Voltage and current at Infinite bus and fuel cell.

CHAPTER 5

CONCLUSIONS AND FUTURE SCOPE OF WORK

5.1 CONCLUSIONS

In this thesis, two renewable electric generation systems namely micro turbine (MT) system and fuel cell (FC) system has been studied. The detailed dynamic model of each of the system component has been developed and the system models are implemented under SIMULINK environment. The micro turbine operation during initial motoring and thereafter generating mode has been studied. The performance during grid connection and islanding has also been studied. The active and reactive power variation for the connection of fuel cell system with ac utility has been studied. The following conclusions are drawn from this study:

- Very small duration transients are observed when the micro turbine operation is changed from grid mode to islanding mode. Further, during islanding, the line current of permanent magnet synchronous machine is high.
- The microturbine initially operates in motoring mode before attaining the generating mode operation.
- With the flow of hydrogen on electrolyte, the hydrogen and oxygen pressure increases but water vapor pressure decrease. However, the trend reverses after some time.
- The control is effective in providing sinusoidal voltage at fuel cell terminals.

5.2 SCOPE FOR FUTURE WORK

The followings are identified as the scope of further work

- The interface of the REGS has been considered as ac system. The performance of the systems can be studied for other interface like isolated mode supplying consumer load, HVDC link.
- The performance has been studied while each system is working independently. The integration of these systems and the integration of these systems with other REGS shall be investigated.

REFERENCES:

[1] T. E. Hoff, H. J. Wenger and B. K. Farmer, "Distributed generation: an alternative to electric utility investments in system capacity" Energy policy, Vol. 24, No. 2, pp. 137-147, 1996

[2] T. Ackermann and V. Knyazkin, "Interaction between distributed generation and the distribution network: operation aspect" IEEE/PES Transmission and Distribution Conf. and Exhibition 2002: Asia Pacific, Vol. 2, 6-10 Oct. 2002, pp. 1357-1362, Yokohama, Japan

[3] M. T. Doyle, "Reviewing the impacts of distributed generation on distribution system protection" Power Engineering Society Summer Meeting, 2002 IEEE, Chicago, USA, Vol. 1, 21-25 July 2002, pp. 103-105

[4] P. P. Barker and B. K. Johnson, "Power system modeling requirements for rotating machine interfaced distributed resources" Power Engineering Society Summer Meeting, 2002 IEEE, Chicago, USA, Vol. 1, 21-25 July 2002, pp. 161-166

[5] P. P. Barker and R. W de Mello, "Determining the impact of distributed generation on power systems: Part I. Radial distribution systems" Power Engineering Society Summer Meeting, Seattle, Washington, USA, 2000 IEEE, Vol. 3, 16-20 July 2000, pp. 1645-1656

[6] F. V. Edwards, G. J. W. Dudgeon, J. R. McDonald and W. E. Leithead, "Dynamics of distribution networks with distributed generation" Power Engineering Society Summer Meeting, Seattle, Washington, USA, 2000 IEEE, Vol. 2, 16-20 July 2000, pp. 1032-1037

[7] In-Su Bae, Jin-O Kim, Jae-Chul Kim and C. Singh, "Optimal operating strategy for distributed generation considering hourly reliability worth" Power Systems, IEEE Transactions on, Vol. 19, No. 1, February 2004

[8] A. G. Amendola and M. C. Rocha, "Fuel cell plant-a proposed analysis for economical feasibility of implantation" Electricity Distribution, 16th Int. Conference and Exhibition on, Amsterdam, the Netherlands, 18-21 June 2001, Part 1, (IEE Conf. Publ. No. 482), Vol. 4

[9] C. Haynes and W.J. Wepfer, "'Design for power' of a commercial grade tubular solid oxide fuel cell" Energy Conversion & management, Vol. 41, Issue 11, July 2000, pp. 1123-1139

[10] D. J. Hall, and R. G. Colclaser, "Transient Modeling and Simulation of a Tubular Solid Oxide Fuel Cell," IEEE Trans. Energy Conversion, vol. 14, Issue 3, pp. 749-753, September 1999.

[11] D. Singh, D. M. Lu and N. Djilali, "A two-dimensional analysis of mass transport in proton exchange membrane fuel cell" International Journal of Engineering science, Vol. 37, Issue 4, March 1999, pp. 431-452

[12] Bagnasco, B. Delfino, G.B. Denegri and S. Massucco, "Management and dynamic per-formances of combined cycle power plants during parallel and islanding operation" Energy Conversion, IEEE Transactions on, Vol. 13, No. 2, June 1998

[13] Borghetti, G. Migliavacca, C. A. Nucci and S. Spelta, "Black-startup simulation of a repowered thermoelectric unit" IFAC Symposium on power plants & Power Systems Control, 26-29 April, 2000, Brussels, Belgium, pp. 119-126

[14] Amer Al-Hinai and Ali Feliachi, "Dynamic model of a microturbine used as a distributed generator" System Theory 2002, Proceedings of the 34th Southeastern Symposium on, Huntsville, Alabama, 18-19 March 2002, pp. 209-213

[15] W. G. Scott, "Micro-Turbine Generators for Distribution Systems," IEEE Applications Magazine, Vol. 4, Issue 4, pp. 57-62, May/June, 1998.

[16] Peter A. Daly and Jay Morrison, "Understanding the potential benefits of distributed gen-eration on power delivery systems" Rural Electric Power Conference, 29 April-1 May 2001, pp. A2-1–A2-13, Little Rock, Arkansas, USA

[17] A. Agustoni, M. Brenna, R. Faranda, E. Tironi, C. Pincella and G. Simioli, "Constraints for the interconnection of distributed generation in radial distribution systems" Harmonics and Quality of Power, 10th International Conference on, Vol. 1, 6-9 Oct. 2002, pp. 310-315, Rio de Janeiro, Brazil

[18] W. I. Rowen, “Simplified mathematical representations of heavy duty gas turbines,” Journal of Engineering for Power, Transactions ASME, vol. 105, no. 4, pp. 865-869, Oct, 1983.

[19] L. N. Hannet and Afzal Khan, “Combustion turbine dynamic model validation from tests,” IEEE Transactions on Power Systems, vol. 8, no. 1, pp. 152-158, Feb. 1993.

[20] Working Group on Prime Mover and Energy Supply Models for System Dynamic Performance Studies, “Dynamic models for combined cycle plants in power system studies,” IEEE Transactions on Power Systems, vol. 9, no. 3, pp. 1698-1708, August 1994.

[21] A. Cano, F. Jurado and J. Carpio, “Influence of micro-turbines on distribution networks stability,” in Proceedings, IEEE PES General Meeting, vol. 4, pp. 2153-2158, Jul. 2003, Toronto, Canada.

[22] Francisco Jurado and Jose Ramon Saenz, “Adaptive control of a fuel cell microturbine hybrid power plant,” IEEE Transactions on Energy Conversion, vol. 18 no.2, pp. 342-347, June 2003.

[23] Amer Al-Hinai and Ali Feliachi, “Dynamic model of a microturbine used as a distributed generator,” in Proceedings, 34th Southeastern Symposium on System Theory, Huntsville, pp.209-213, Alabama, March 2002.

[24] Bimal K.Bose, Modern Power Electronics and AC Drives, Pearson Education, 2003.

[25] J. Padulles, G. W. Ault, and J. R. McDonald, “An Approach to the Dynamic Modeling of Fuel Cell Characteristics for Distributed Generation Operation,” IEEE-PES Winter Meeting, vol. 1, Issue 1, pp. 134-138, January 2000.

[26] D. N. Gaonkar and R. N. Patel, “Modeling And Simulation Of Microturbine Based Distributed Generation System”, Proceedings of IEEE Power India Conference, New Delhi, pp. 5, April, 2006

[27] K. Sedghisigarchi and A. Feliachi, “Dynamic and Transient Analysis of Power Distribution Systems with Fuel Cell-Part I: Fuel-Cell Dynamic Model,” IEEE Trans. Energy Conversion, vol. 19, Issue 2, pp. 423-428, June 2004.

[28] C. Wang and M. H. Nehrir, "A Physically-Based Dynamic Model for Solid Oxide Fuel Cells," accepted for IEEE Trans. Energy Conversion September 15, 2006.

[29] C. J. Hatziadoniu, A. A. Lobo, F. Pourboghrat, and M. Daneshdoost, "A Simplified Dynamic Model of Grid-Connected Fuel-Cell Generators," IEEE Trans. Power Delivery, vol. 17, Issue 2, pp. 467-473, April 2002.

[30] S. Stevandic, and J. Jiang, "A Standalone, Reduced-order Model and Control of a Grid-Connected Fuel Cell Power Plant," IEEE-PES General Meeting, vol. 2, pp. 679-686, July 2003.

[31] Z. Miao, M. A. Choudhry, R. L. Klein, and L. Fan, "Study of a Fuel cell Power Plant in Power Distribution System-Part I: Dynamic Model," IEEE-PES General Meeting, vol. 2, pp. 2220-2225, June 2004.

[32] Y. Zhu, and K. Tomsovic, "Development of Models for Analyzing the Load-Following Performance of Micro Turbines and Fuel Cells," Electric Power Syst. Research, vol. 62, Issue 1, pp. 1-11, May 2002.

[33] F. Blaabjerg, Z. Chen, and S. B. Kjaer, "Power Electronics as Efficient Interface in Dispersed Power Generation Systems," IEEE Trans. Power Electronics, vol. 19, Issue 5, September 2004.

[34] J. J. Woo, "Modeling and Control of Fuel Cell Based Distributed Generation Systems," PhD Dissertation, Ohio State University, 2005.

[35] N. Mohan, T. M. Undeland, and W. P. Robbins, "Power Electronics, Converters, Applications and Design," 2nd Edition, John Wiley & Sons.

[36] C. Wang, and M. H. Nehrir, "Short-time Overloading Capability and Distributed Generation Applications of Solid Oxide Fuel Cells," accepted for IEEE Trans. Energy Conversion September 15, 2006.

[37] P. G. Barbosa, L. G. Rolim, E. H. Watanabe, and R. Hanitsch, "Control Strategy for Grid-Connected DC-AC Converters with Load Power Factor Correction," IEEE Proc. Gener. Transm. Distrib., vol. 145, Issue 5, pp. 487-491, September 1998.

[38] D. Georgakis, and S. Papathanassiou, "Modeling of Grid-Connected Fuel Cell Plants," Proc. CIGRE Power Systems with Dispersed Generation, April 2005, Athens.

[39] K. Sedghisigarchi, and A. Feliachi, "Dynamic and Transient Analysis of Power Distribution Systems with Fuel Cell-Part II: Control and Stability Enhancement," IEEE Trans. Energy Conversion, vol. 19, Issue 2, pp. 429-434, June 2004.

[40]Gaonkar, D. N., Pillai, G. N., and Patel, R. N., (2008), Dynamic performance of microturbine generation system connected to grid, *Journal of Elect. Power Compon. Syst.,* Vol. 36, No. 10, pp. 1031–1047, 2008.

[41]Pillai, P., and Krishnan, R., (1989), Modeling, simulation, and analysis of permanent-magnet motor drives, Part I: The permanent-magnet synchronous motor drive, *IEEE Trans. Indl. Appl.,*Vol. 25, No. 2, pp. 265–273, 1989.

[42]Pena, R. Cardenas, R. Blasco R., G. Asher G. and J. Clare J., (2001), A cage induction generator using back-to-back PWM converters for variable speed grid connected wind energy system," in *Proc. IECON'01 Conf.*, vol. 2, 2001, pp. 1376–1381,2001.

[43]Chung, S.-K., (2000), Phase-locked loop for grid-connected three-phase power conversion systems, *Proc. Inst. Elect. Eng.*, Vol. 147, No. 3, pp. 213–219, 2000.